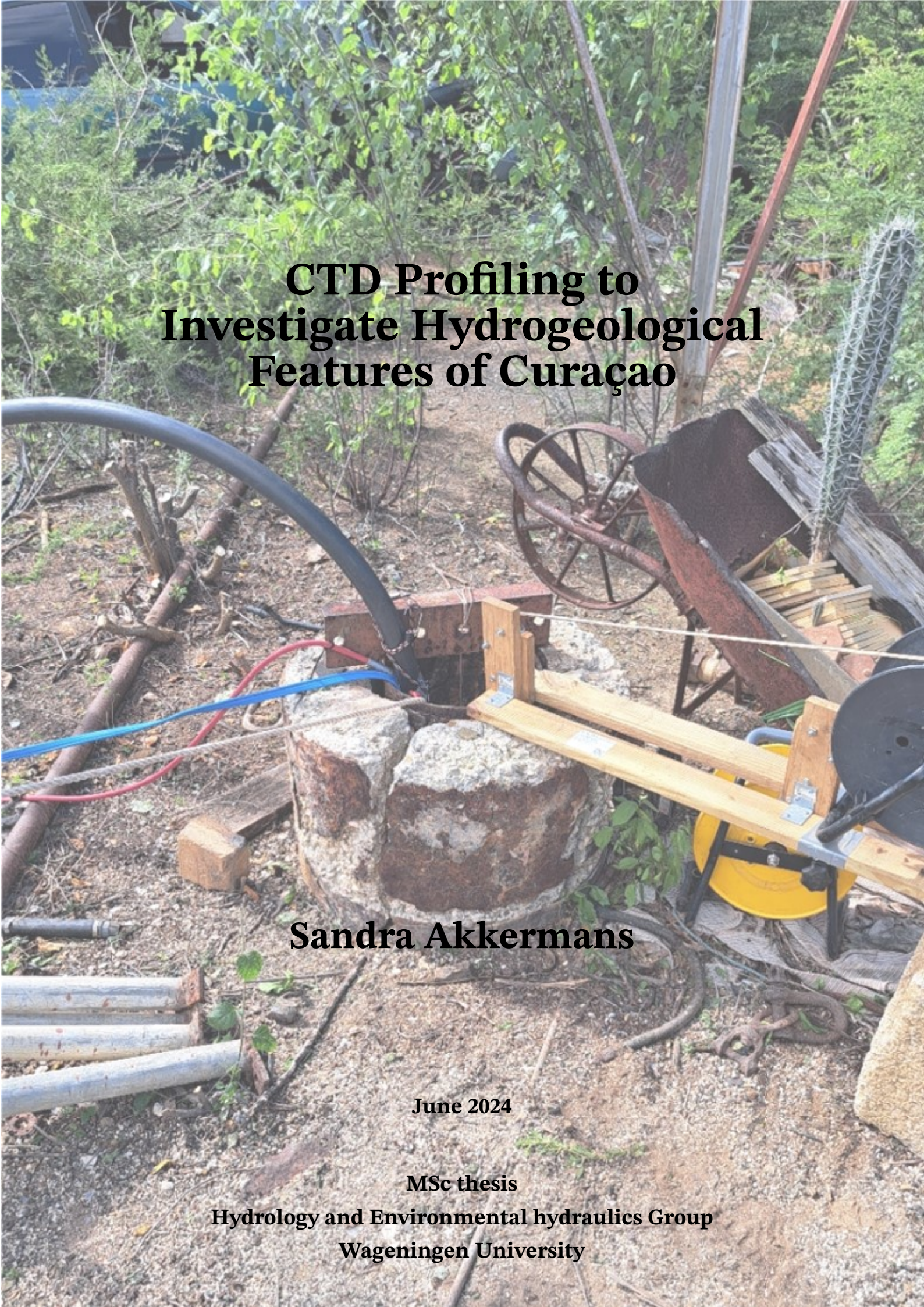

CTD Profiling to Investigate Hydrogeological Features of Curaçao

Sandra Akkermans

June 2024

MSc thesis

Hydrology and Environmental hydraulics Group

Wageningen University

Abstract

This thesis investigates methods for identifying fractures in the geological subsurface of Curaçao using CTD profiles and other temperature measurements during pump tests. Deviations from the background profile in different tracer pump tests, natural salt tracer tests within wells with non-uniform EC profiles and point source heat injection tracer tests, were analyzed to characterize subsurface fractures. Results indicate that both temperature and EC experiments reveal comparable fracture depths. Additionally, Star Oddi temperature measurements show potential in detecting fractures, despite the spatial resolution. Static temperature profiles reveal multiple fracture depths, although with some uncertainties. The effectiveness of proposed methods varies, with EC-depth profiles during a natural tracer test proving effective. In wells lacking EC variability, the temperature tracer method with temperature-depth profiles, or Oddi temperature measurements can serve as an alternative. Also, the heterogeneity of the subsurface of the Curaçao island has become apparent from the results, with also having different fracture distributions in depth throughout the different measured wells. Further enhancement of measurement methods, including increased Oddi temperature measurement density, multiple heat injection depths and averaging of multiple static profiles as background value, could improve accuracy.

Contents

1 | Introduction

Curaçao is one of the Antilles islands in the Caribbean Sea. It is known for the high-quality coral reefs on the southwest side of the island. Coral reefs provide economic advantages for Curaçao through tourism and fishing and also give protection from storms and flooding [Eddy et al., 2021]. In the past 40 years, a 50% decline of coral reefs in the Caribbean has been observed, with a projection that in the next few decades, 60% of present coral will be lost if the present rates continue [Waitt institute, 2017]. Currently, the coral reefs experience multiple stressors from the environment such as climate change. Where pollution and sedimentation also form a problem [Lesser, 2021]. This pollution or sedimentation can be caused by submarine groundwater discharge (SGD), which could contain pollutants deposited onshore [Liu and Du, 2022]. High levels of SGD with high amounts of nutrients negatively affect coral survival, but lower levels can have a positive effect [Lubarsky et al., 2018]. This is due to the possible nutrient load of SGD, which differs in amount with these levels of SGD. As this is an important factor for coral management it is important to understand where and how the groundwater is flowing on and through the island.

The SEALINK project is an overall research for the effects of the environment on the growth of the coral around Curaçao. Part of this project is the research of the effects of SGD and to look at the relationship with the sea and land processes [Sealink]. This project is set out to look at the survival and growth of the coral reefs of the Dutch Caribbean. The groundwater that is part of the SGD flows out of the different geologies of Curaçao. The different geological formations present on the island (Figure 1.1) have different transmissivities [Abtmaier, 1978] as the they are formed under different conditions, which is believed to have a big impact on the SGD. Fractures within a formation also have a critical role in groundwater flow [Singhal and Gupta, 2010]. Fractures form in a rock due to stress. These fractures can give space for water to flow through, though this is only possible when they are in a network. This connectivity causes the flow to go in another direction than originally in a case without fractures, this is illustrated in figure 1.2 as water can be directed by the direction of a fracture, depicted with the blue arrows. Also, other features could be present, for example wells or faults,

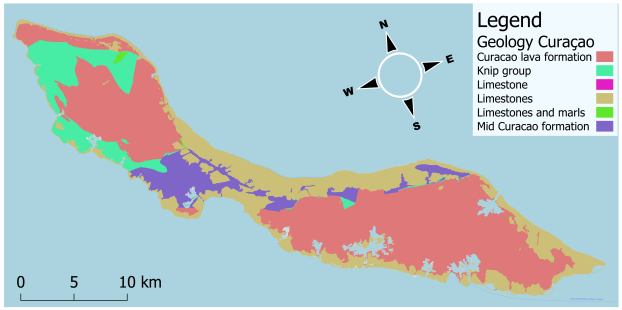

Figure 1.1: Geology of Curaçao (logged by Beets [1972])

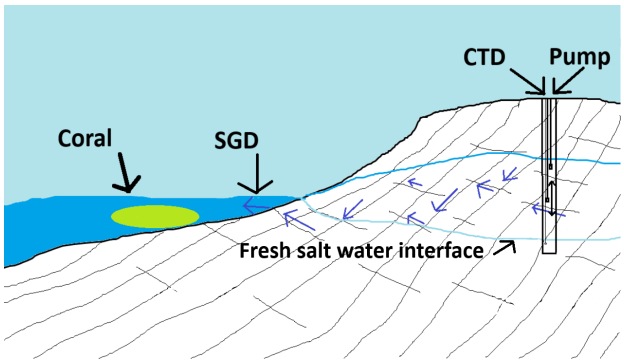

Figure 1.2: Schematic depiction of the role of fractures on groundwater flow together with an indication of the experiment in a well and an idea of how SGD flows into the sea to the coral (blue arrows).

were wells in itself can form conduits of groundwater [Gailey, 2017]. As these subsurface features are an important factor in the SGD it is good to have an insight in the fracture distribution in these geologies.

To see where features are located in a well, conductivity temperature depth (CTD) profiles were taken. These are profiles in the saturated zone of a borehole and depict the conductivity and temperature of the water in depth. As Curaçao is an island, it has a freshwater lens on top of saline water [Post et al., 2018] where salt is present in the bottom of a well and the fresh and salt interface is within the water column of a well (Figure 1.2). Former studies of electrical conductivity (EC) in wells of Curaçao by Rowbottom and Winkel [1979] however show that the distribution of salt in the groundwater does not have a linear relationship with distance from the coast (Figure 1.3). Where seawater on average has a conductivity of 50.000 μS/cm and drinkable water a

maximum of 1.000 μS/cm [Walton, 1989]. So, to get a better insight in this groundwater system of the island, a CTD study was used. CTD-profiles could potentially tell something about the structures in the subsurface, which influence this salt distribution. Static profiles will be examined, to see whether this can be used as fracture indicators in a well or that pump tests are required to examine this. Poulsen et al. [2019] presents a method to detect subsurface features in a well. This by injecting a salt concentration in the bottom of the well and pumping at the top. With this, the pumping will create a salt profile throughout the whole water column. At depths where this process creates a different gradient in the profile than the background profile, a fracture is likely to be present. This gradient can be present due to a subsurface flow through fractures containing fresher water. As stated by Poulsen et al. [2019], the experiment can also be done using other tracers. For this research also a temperature injection experiment was conducted. This type of experiment can also be done in wells with a uniform EC profile. Read et al. [2015] uses a point heat injection as tracer, where they measure the speed and quantity of the heat dispersion upwards in a well to acknowledge features in a well. By doing this the reaction of the water column by the pump can be measured and analysed. In this research these two tracer methods will be handled with some alterations, where for the salt tracer test the present salt concentration in the wells is assumed to act as a natural tracer, in contrast to adding this separately. Where for the temperature tracer test different measuring devices will be used as opposed to the fibre optic DTS (distributed temperature sensing) measurement done by Read et al. [2015]. This to see if this is a viable cost-effective option, and whether these heat point injection tracer tests can provide essential information about the well's fractures.

1.1 Context

The project of which this thesis is part of is a PhD linked to the bigger project called SEALINK. This project aims to investigate the effect of terrestrial inputs on the island of Curaçao on near shore coral reefs. Where Titus Kruissen is investigating the scope of water flow from and on the island towards these coral reefs. For this project a more detailed look on the local fracture and subsurface flow in wells is taken. Therefore this thesis will be supportive to the overall SEALINK project.

1.2 Research questions

The objective of this research is to characterise the hydro-geological situation and features in wells on the island of Curaçao. To meet the research objectives the following research questions will be answered. With questions:

- How can hydro-geological features be characterised out of measured CTD-profiles around a conducted pumping test?
- To what extent is this possible from static CTD-profiles?
- Which fracture quantifying method is best for coastal rock formations?

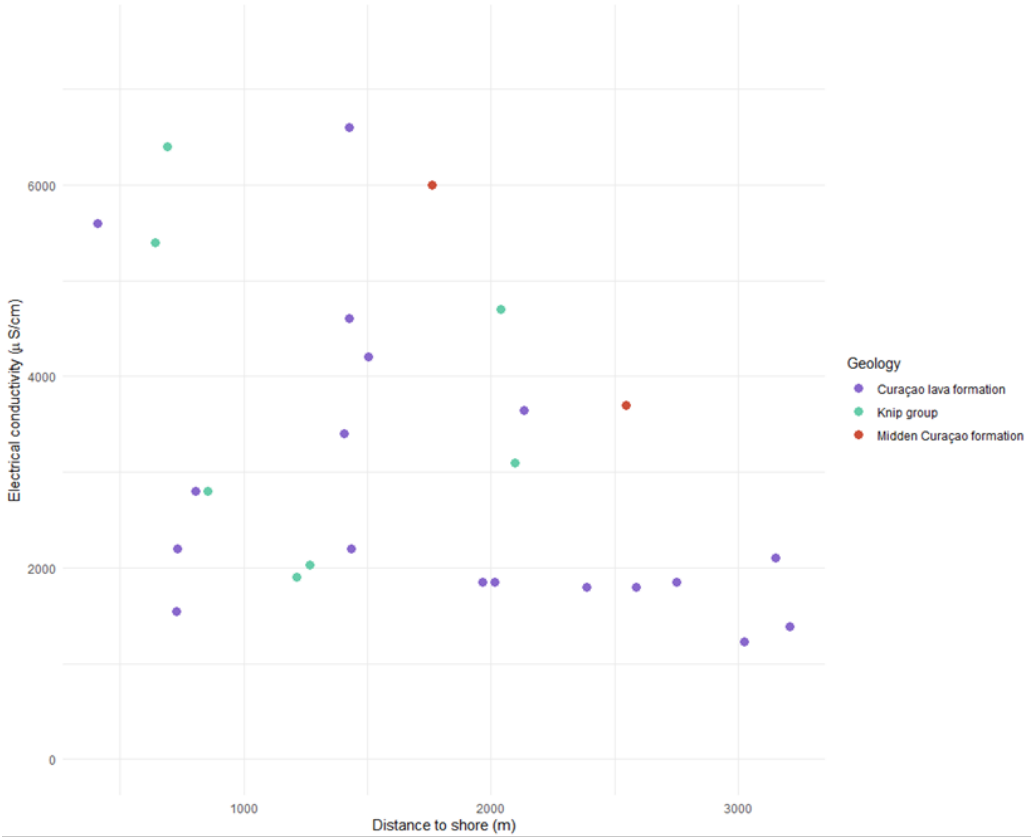

Figure 1.3: Electrical conductivity at sea level in wells measured by Rowbottom and Winkel [1979] plotted against distance to the shore. The colors indicating the different geological formations the wells where situated.

2 | Field site and data

2.1 Geology and climate

The island of Curaçao consists of different geological layers. The biggest part of the island is made up of the Curaçao lava formation (Figure 1.1), this was formed in the sea where lava meets sea water [van Buurt, 2009]. The pillow like structure can also have some basalt intrusions that formed when magma found it's way through the "pillow" structures and cooled slower. This formation has been pushed up due to tectonics and thus emerged from the sea. During the process of emerging from the sea a limestone rock formed on top of this formation due to calcareous sediments that accumulated on the basalt base. These rocks are mostly present at the edges of the island. The Knip formation seen in the north-west in figure 1.1 is a sedimentary rock formed out of sands, clays and silicates. The Midden Curaçao formation consists of sand- and mudstones with regionally conglomerates. The hydrogeology of these geological formations is diverse, as the basalt formation can have transmissivities of 50 to 200 m^2/day where the Knip formations and midden Curaçao formation can have 5 m^2/day [Abtmaier, 1978]. This can have big impacts on the SGD as the groundwater will flow faster through the basalt layers than through the Knip formation.

The topography of the island is hilly with the highest point at 372 meters. As it is an island the fresh-water source is precipitation. The island has a tropical climate where average day temperatures do not differ more than 10 degrees Celsius over the year, with an average temperature of 27 degrees Celsius. The amount of precipitation accompanying this climate is not homogeneous throughout the year, but has an average annual value of 550 mm. In the beginning of the year it is dry for a few months, and in the end of the year in the months of October, November and December it is wetter with monthly around a hundred millimeters of rain (Figure 2.1) [Martis et al., 2002, Meteorological Department Curaçao].

In prior research Abtmaier [1978] stated that at the end of the dry season the groundwater showed an increase of conductivity of 20%. In areas where they pumped the irrigation water in high quantities this increase could even be 50%. Thus salt water intrusion can form a problem for places with extensive pumping. For this

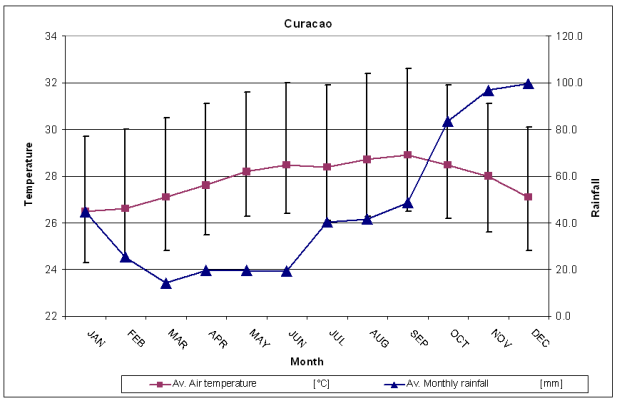

Figure 2.1: Climate summary of Curaçao. Retrieved from Meteorological Department Curaçao.

project EC (Electrical Conductivity) depth profiles were taken, where Rowbottom and Winkel [1979] have already done this for some places. The existing profiles are all taken as a static profile, in this research profiles throughout a pumping test were taken to get a better look at the present features in the subsurface. Simultaneously, temperature depth profiles were taken. The profiles were taken with a CTD (Conductivity Temperature Depth) logger, which measures the electrical conductivity, temperature and pressure.

2.2 Field sites

All wells measured in this study were uncased, which implies that the water in the wells directly are at contact with the surrounding subsurface. The fieldwork is done together with a master thesis student (Joshua Leusink) who has conducted pump tests in the same wells. The measurements were taken in 11 different places on the island, as seen in figure 2.2.

Well 1 is located next to some farm fields almost at the West point of the island. It lies within the Curaçao lava formation and is within 0.4 km of the coast. Where well 2 also lies in the West of the island it is within the Knip group formation and a bit further from the coast (2.3 km). This well is within a military area which is used as practice fields, and no agriculture around. Well 3 is again within the Curaçao lava formation and with 1.4 km also close to the coast. The well is located within a nature reserve where the well is sometimes used to irrigate the vegetation. Well 4 and 5 both lie within the

Table 2.1: Distance to shore and height above sea level of each measured well.

Well	Distance to coast (km)	Elevation (m)
1	0.4	18
2	2.3	27
3	1.4	11
4	3.2	69
5	2.3	21
6	3.4	28
7	3.3	17
8	3.5	21
9	2.3	31
10	2	39
11	3.2	27

Midden Curaçao formation and respectively 3.2 and 2.3 km from the coast. the surrounding land use is mostly shrubs and houses where well 4 is only used to water palm trees, as the water contains salt and the other vegetation around can not withstand this amount of salt, and well 5 has not been used for decades. Well 6 is an unused well in the backyard of a house near well 7. The neighbourhood lies a bit higher than well 7, with a height difference of 11 meters between well 6 and 7. Well 7 is located near a field which is used as a community farming facility. In the months outside of the rain-season when their water basins are empty this well is used as pumping well for irrigation. The water basin is located around 150 meters from the well and is in the form of a round silo. Also, at almost 500 meters distance a dam is located which fills when big rain events occurred. Which at the time of the pump test the dam was filled with water. Furthermore, the well is located in the middle of the island and approximately 1.7 km from the Piscedera bay or 3.3 km from the sea at 17 meters above sea level. Well 8 is located in an area of the government which at the measurement time did not get used for intensive agriculture. Near the well a few lakes are present within 100 meters. The well lies within the Curaçao lava formation, 3.5 km from the sea and 1.6 km from the bay named Schottegat. Well 9 is located in cattle fields of a farmer, occasionally containing sheep. No active pumping is done in this well throughout the year. The location of the well is at the edge of the Curaçao lava formation next to the limestone formation and approximately 2.3 km from the sea at 31 meters above sea level. Well 10 is a well in an agricultural field which is not used to pump water. It is located near well 9, has a distance of 2 km to the sea and lies within the Curaçao lava formation. Just as most of the wells, does well 11 lie within the Curaçao lava formation, it is situated in a backyard and lies 3.2 km from the sea. Behind the backyard a natural area is located which stretches to the coast. The elevation of the wells shown in figure 2.2 are given in table 2.1 just as the mentioned distances to the coast.

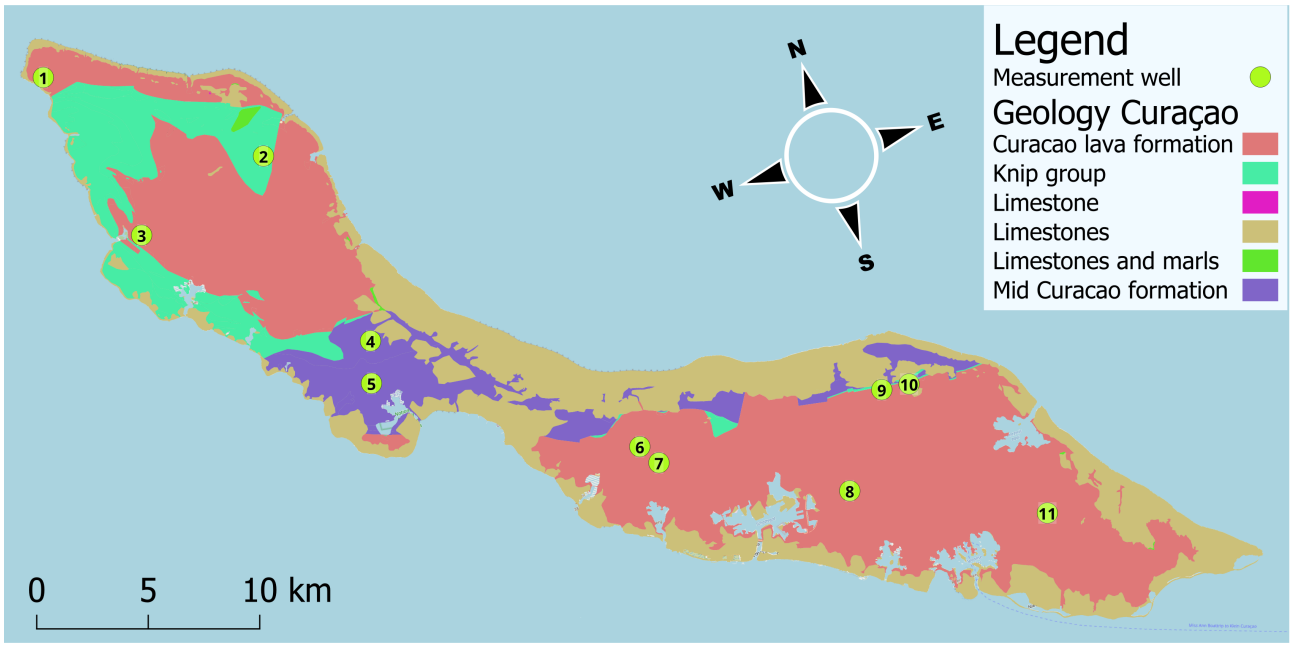

Figure 2.2: locations of pump tests and analysed wells. In the background the geological map of Curaçao (Beets [1972]).

3 | Methodology

The main methods used in this research are electrical conductivity and temperature profile measurements in wells on the island of Curaçao. Additionally, profiles were taken before, during and after conducted pumping tests with tracers, this in order to see the response in salinity and temperature. In this methodology chapter firstly, the general set-up of the pumping test will be explained, secondly the measurements done during these tests will be shown and lastly the analysing methods will be described.

3.1 Main measurement plan

For this study the fieldwork plan is based on multiple hydro-geological measurement methods. This by combining already existing methods and adapting it to a version applicable in fractured coastal rock formations. With these methods fracture locating and transmissivity studies have been conducted. A natural and induced tracer test was executed together with a pumping test in single-well experiments. This is done around the island of Curaçao on different geologies and locations, with various well depths and widths. Next to these measurements, also static (without active pumping) Conductivity Temperature Depth profiles (CTD-profiles) were taken to compare with the dynamic (with active pumping) experiments.

As a base of the experiment a pump test is conducted. Here, the pump was placed a few meters under the water level in the well (Figure 3.1 and number 4 in Figure 3.2). The pumping rate depended on the pre-assumed transmissivity which was at least low enough so that the well would not be emptied out at the start of the test. The pumped water was discharged through a pipe of either ten or twenty meters from the well, in a lower elevated location. Which was done to diminish return flow to the well. Further work on the drawdown data from the pumping tests are done in the master thesis of Joshua Leusink [Leusink, 2024].

3.1.1 CTD profiles

CTD profiles can be measured in a static (no active induced flow) well, a pumped one, or with induced gradients [Smart and Worthington, 2003]. In this study, both static and directly pumped profiles were taken. The

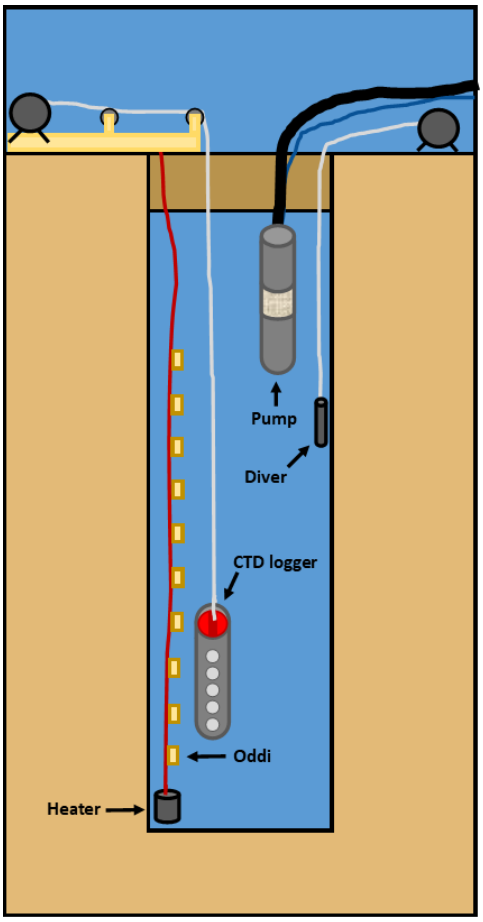

Figure 3.1: Schematic depiction of measurement set up

RBR brevio^3 (Figure 3.4), which is the CTD-logger that was used was attached to a cord that was marked at every meter. This device has a measurement interval of every 0.5 seconds and measures with an accuracy of +/- 3 µS/cm for the conductivity and +/- 0.002 °C for the temperature. The cord with marks was winded up on a reel to know at what depth was being measured (Figure 3.1 and Figure 3.2 number 1). The logger also measures depth by pressure, so when continuously logging the water level in the well, the exact depth of these profiles could be determined. The logging of the water level was done by a pressure diver which was placed below the pump, and a dipper to periodically measure the water level by hand as a check (Figure 3.1 and Figure 3.2 number 3 and 6 respectively). To make sure the CTD logger was safely hanging in a well, a protective case was built to hang around the logger. A PVC pipe was cut to size and holes were drilled all around so that water would still run through to measure but so that the

Figure 3.2: Set up of pump test with tracer measurements. With the numbers depicting: 1) rope reel CTD (Conductivity Temperature Depth) logger 2) pulley system 3) rope reel diver 4) pump tube and electrical cord 5) cord heater and oddi line 6) dipper

Figure 3.3: Casing used around the CTD-logger to protect from potential damage made to the RBR Brevio by the well wall

Figure 3.4: The used CTD-logger, it is a RBR Brevio[3]

logger would not bump against the sides (Figure 3.3). To provide a smooth running of the cord a pulley system was created to also prevent potentially breaking the cord on the side of the well (Figure 3.1 and Figure 3.2 number 2). The logger is lowered and raised in the well throughout the pump test. Depending on the width of the well, this was done for the whole depth or only beneath the pump when the well was too narrow to fit both the pump and logger. Some wells are not wide enough for the CTD logger, pump, and electrical cord to fit all next to each other. In these wells either a CTD diver, which is smaller, was used instead of the RBR Brevio[3] logger, or only the water column beneath the pump was measured.

During the pump test, a time interval was set to roughly measure at a constant interval. For the first few tests this interval was every thirty minutes but after looking at the results, fifteen minutes was chosen as a more suitable interval. A set depth was chosen per test to rest the CTD-logger in the time between the profiles. This was done as a backup water level logger and to keep the logger from drying out covered in salty water.

3.1.2 Tracer experiments

Poulsen et al. [2019] injected a constant rate of salt at the bottom of the well with their tracer tests. This is not possible to reproduce in the scope of this research, but as the island of Curaçao has a freshwater lens on top of salt water, salt is already present at the bottom of most wells. In this case, a well with a gradient of EC values may function similarly. Here, salt is thus already present at the bottom of the well, which can be pumped up to hypothetically create the same effect of the injection experiment. The background concentration is important to consider, as there is already salt in the well that is affecting the water column, which is not the case in the wells from Poulsen et al. [2019]. This experiment

Figure 3.5: Star oddi, Temperature measuring device

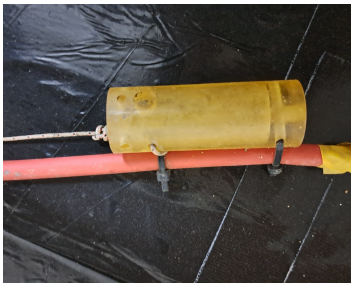

Figure 3.6: Star oddi casing, attached to cord of heater with spacing of one meter from each oddi

is only possible in wells where there is not a uniform EC profile.

In wells with a uniform EC profile the method of Read et al. [2015] can be used, with some simplifications as fibre optic measurements where not available. To measure the temperature in a profile next to the CTD profiles taken, ten Star-Oddi temperature probes (Figure 3.5) were lowered in the well in a sequence (Figure 3.1). These were spaced from each other on a line with one meter between each Star-Oddi with a casing to hold them (Figure 3.6). In this way, we had a constant temperature measurement at 10 fixed depths and a full CTD profile every fifteen minutes. A heating element (2000 Watts) was placed close to the bottom of the well, which functioned as the tracer injection point with the Star-Oddi's above it (Figure 3.1). The heater was heating for 15 minutes in each test after at least half an hour of pumping. When heating the water, the heat transfers up, either by the pump, in-well conduit current between two fractures [Maurice et al., 2011] or convection. Before the heating and pumping a background CTD profile is taken.

3.2 Analysis

The aim of the analyses is to see whether the proposed methods are fit to find fractures in the subsurface of a fractured coastal rock.

3.2.1 Static temperature depth profiles

Bredehoeft and Papaopulos [1965] provides a method of calculating the vertical velocity of the groundwater in wells. This method can only be used in profiles that is depicting a geothermal imposed temperature gradient from the bottom with influence from surrounding water flow creating curves in the profile. In these profiles the effect of surface warming is not part of analyses as in this case the influence from surrounding flows is not the only forcing on the water temperature. Here the surface warming is the main warming force at the top and the geothermal heat the main warming force from the bottom which creates an inflection point. The depths above this inflection point should be neglected in the analyses done with the Bredehoeft and Papaopulos [1965] curves. The curves in the profile can be quantified by fitting it to the Bredehoeft curve (Figure 3.7) which is used to describe the vertical flow in a steady -state situation. The sections of which show a convex or concave structure in the profile below the inflection point in a static temperature profile were super imposed on the curves presented in figure 3.7 with variables being used as presented in figure 3.8, where on the y-axis the depth of measurement is divided by the total length of the vertical section that is examined and on the x-axis the function of f(β, z/L). Where the function is given in equation 3.1:

$$(Tz - T0)/(Tl - T0) = f(\beta, z/L) \tag{3.1}$$

Where the best fitted β value is given as output value. The velocity within the well is then calculated by using equation 3.2.

$$v_z = \kappa\beta/c_0\rho_0 L \tag{3.2}$$

Where $\kappa = 8.368$ x 10^{-3}J/cm°C, $c_o\rho_0 = 4.184$ J/cm^3°C, L the length of the section in cm and β which is unit less (Bredehoeft and Papaopulos [1965]). Here a positive velocity indicates downwards movement and negative upwards. In this way the ambient flow of the in-well water can be calculated.

3.2.2 Static electrical conductivity depth profiles

For characterization of fractures in static EC-profiles, the profiles can be analysed for steps in EC concentration (Saxena et al. [2005]). At depths where a shift in EC is shown the influence of interaction with water from the surrounding fractures is depicted. Next to using the

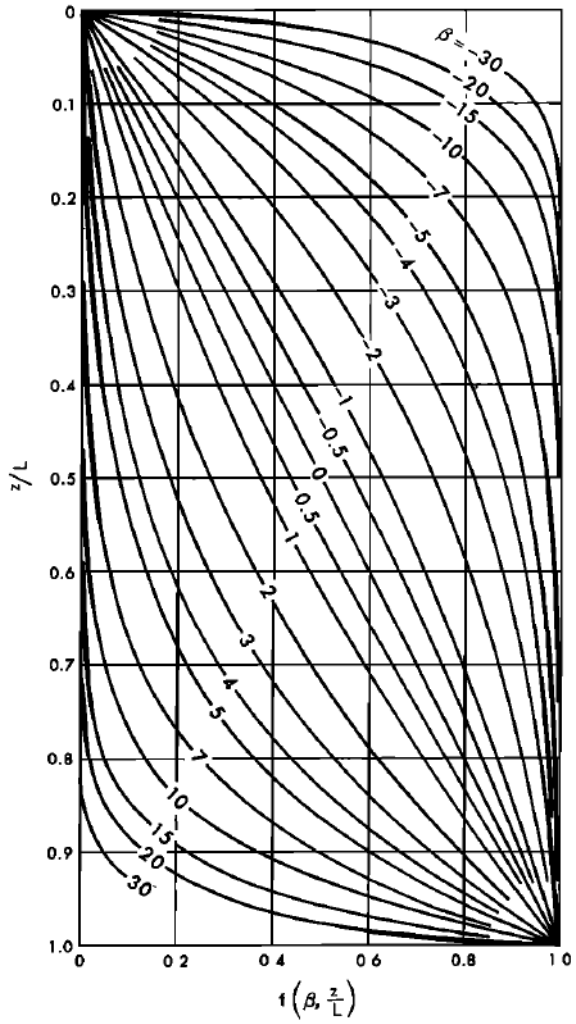

Figure 3.7: The Bredehoeft curves, it shows the relation between depth difference fraction and the temperature difference fraction of the selected area [Bredehoeft and Papaopulos, 1965]

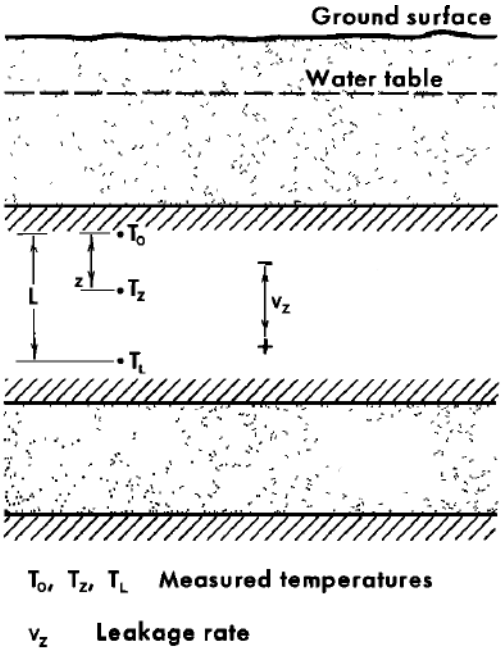

Figure 3.8: Variable diagram for the calculation of the Bredehoeft and Papaopulos [1965] curve's

method of Bredehoeft and Papaopulos [1965] this could also be done for temperature profiles, where temperature differences in surrounding fractures influences the temperature of the water in the well.

3.2.3 Pumptests

A few steps are taken in order to analyse the CTD-profiles taken during a pump test. First, the depths measured by the CTD-logger need to be converted to the correct depth by combining it with the continuously measured water level from the diver. This is important as the CTD-logger measures its depth by pressure and during a pump test the water level varies. The profile logging data will be plotted next to the data from the Star-Oddi's. Because the CTD-logger measures every half a second, the depths are not perfectly at an interval of 0.1 meter. The profiles were integrated over depth with steps of 0.1 meters, in this way every profile can be compared to profiles from the same pump test. As the temperature changes during a test the specific EC will be used in the analysis as this compensates for the temperature difference. For the analyses the difference from the first measurement of the well will be calculated and shown. In the case of the profiles from the CTD-logger, this is done with the first full profile and for the Star Oddi temperature data with a time instance before turning on the pump.

The profiles and Star Oddi temperature data can be plotted with depth on the y-axis and time on the x-axis with the temperature or specific EC as color. In these plots with temperature the proposed heat plume caused by the heating can be followed by finding the maximum temperatures in each profile or in case of the Star Oddi's at each depth. Poulsen et al. [2019] used a method were the speed between these maximums can be calculated by dividing the depth difference by the time that past. This can then be converted to liter per minute by adding the width of the well. Also the heat maps created can be used as a visual analyses of where lateral inflow causes stagnation of the heat plume going upwards. These areas indicate a subsurface feature in the well. This can also be done with the specific EC profiles.

4 | Results

The chapter starts with analyses of the static CTD profiles and the temperature profile analyses with the Bredehoeft curves. This is not done for wells 1, 2 and 4 as no data is present or formatted differently which due to time limits where not analysed. Afterwards, the pump test data will be presented. Pump tests were done in 11 locations (Figure 2.2), where for this result section two will be used: well 7 and 9. This due to time constraints, data insufficiency or lacking of concluding relevance. For figures from the other locations the appendix B can be consulted.

4.1 Static CTD profiles

In this section the static profiles taken before the pump tests will be presented. They will be analysed to what extent fractures can be deduced from the static state of the profiles.

4.1.1 Temperature depth profiles

Static temperature depth (TD) profiles can in some cases tell something about fracture depths as steps in temperature could be present.

For well 3 in figure 4.1, only the depths of 7.5 and 15.5 meters are of interest. At these depths small steps are present which could be fractures, but as it does not have a big step the influence of these fractures are small. In figure 4.2, the temperature depth profile of well 5 is shown. Here at the depths of around 14, 20, 24.5, 36 and 38.5 meters deep a temperature shift is seen. The top three noted depth show a wider step than the bottom two, indicating higher flow velocities within the fractures, thus more weathering at the top than at the bottom.

Figure 4.3 shows a step in temperature at 19 meters deep, suggesting that at that depth a fracture is present as the only feature in this well.

Well 8 shown in figure 4.4 is a shallow well of only 7 meters. Within the profile, when looking at the magnitude of the x-axis, very small temperature changes are present with only a difference of 0.02 degrees Celsius. The one thing to note in this profile is that the biggest difference happens near the bottom of the well, where it gets cooler.

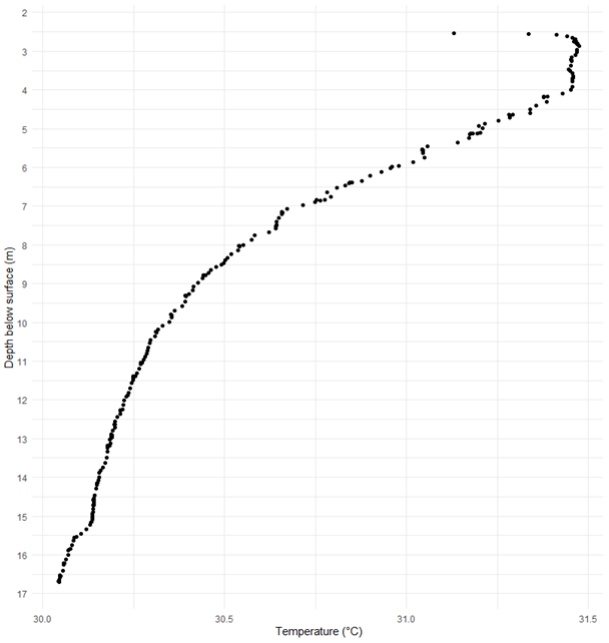

Figure 4.1: Temperature in degrees in depth of well 3.

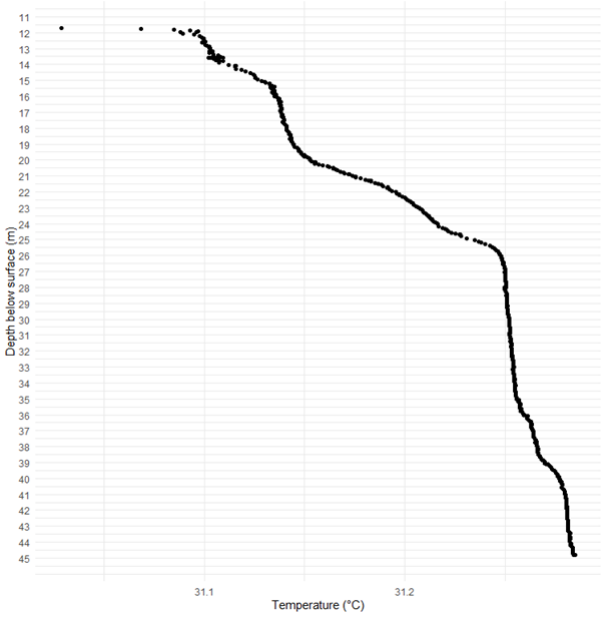

Figure 4.2: Temperature in degrees in depth of well 5.

The TD profile of well 9 (Figure 4.5) has a similar shape than the profile of well 3. In this profile the small step is located around 8.5 meters.

For well 10 in figure 4.6 a clear step is visible around 34 meters and at 13.5 meters deep a sharp turn such as an inflection point is present, only this time it is the other way around, thus not indicating the point of switch from

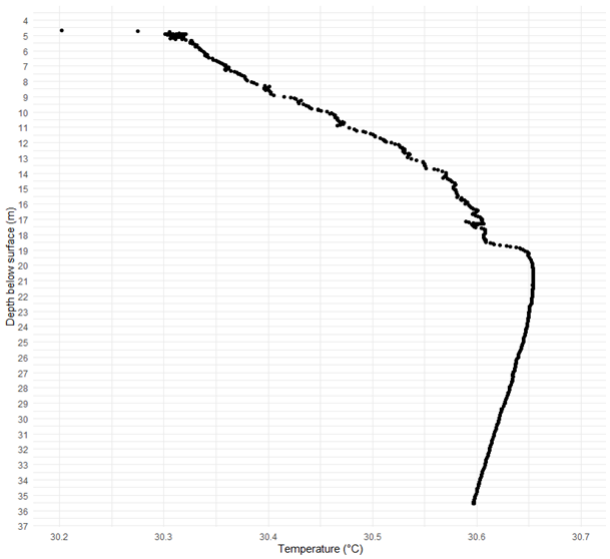

Figure 4.3: Temperature in degrees in depth of well 6.

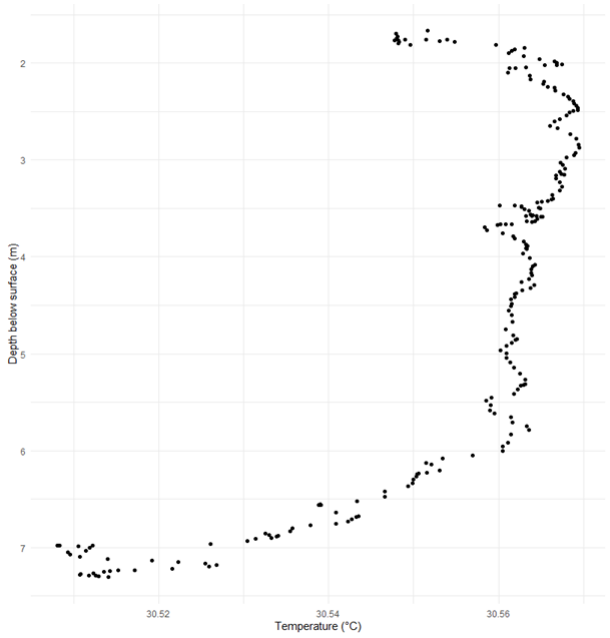

Figure 4.4: Temperature in degrees in depth of well 8.

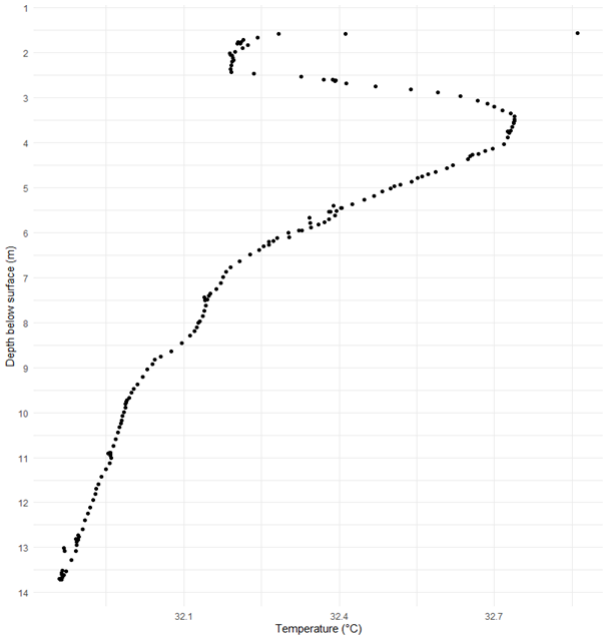

Figure 4.5: Temperature in degrees in depth of well 9.

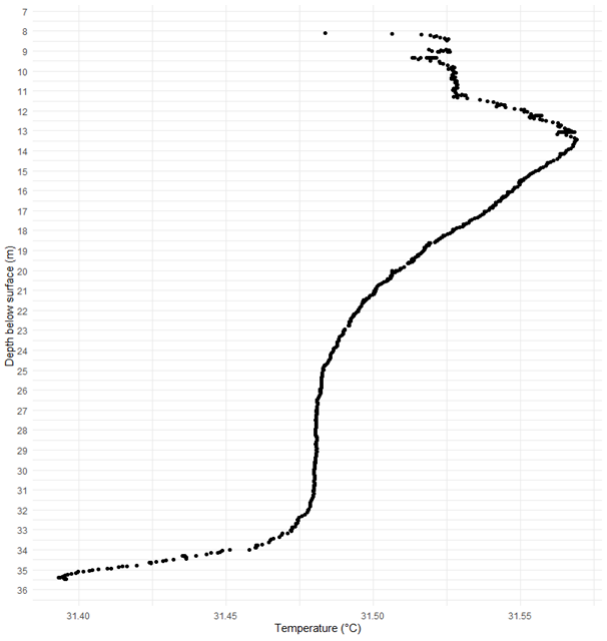

Figure 4.6: Temperature in degrees in depth of well 10.

surface warming to geothermal heat forcing, but indicating a different sort of phenomenon such as a fracture. Well 11, displayed in figure 4.7 shows a step at 19 meters where after the profile shows an inflection point near the bottom of the well. Also, around 10.5 meters a small step is seen in the temperature.

Next the profile of well 7 will be analysed, this is the only measured profile where the method of Bredehoeft and Papaopulos [1965] can be applied, due to the present inflection point noted in section 3.2. In figure 4.8 the profile is presented. The unit less parameter β is given for each part of the profile that shows a convex or concave curve. At 8.8 and 10.7 meters the cumulative flows from the fractures are the highest and thus have the highest lateral influence. Around 11.8, 12.5, 13.5, and 16 meters these flows are the lowest, and for 18.7, 20.3, 21, and 22.5 meters the flow magnitude is around average of the depicted flow rates.

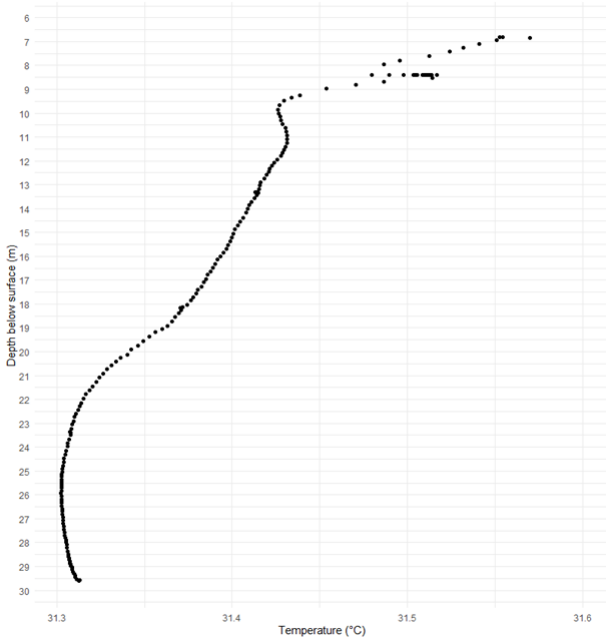

Figure 4.7: Temperature in degrees in depth of well 11.

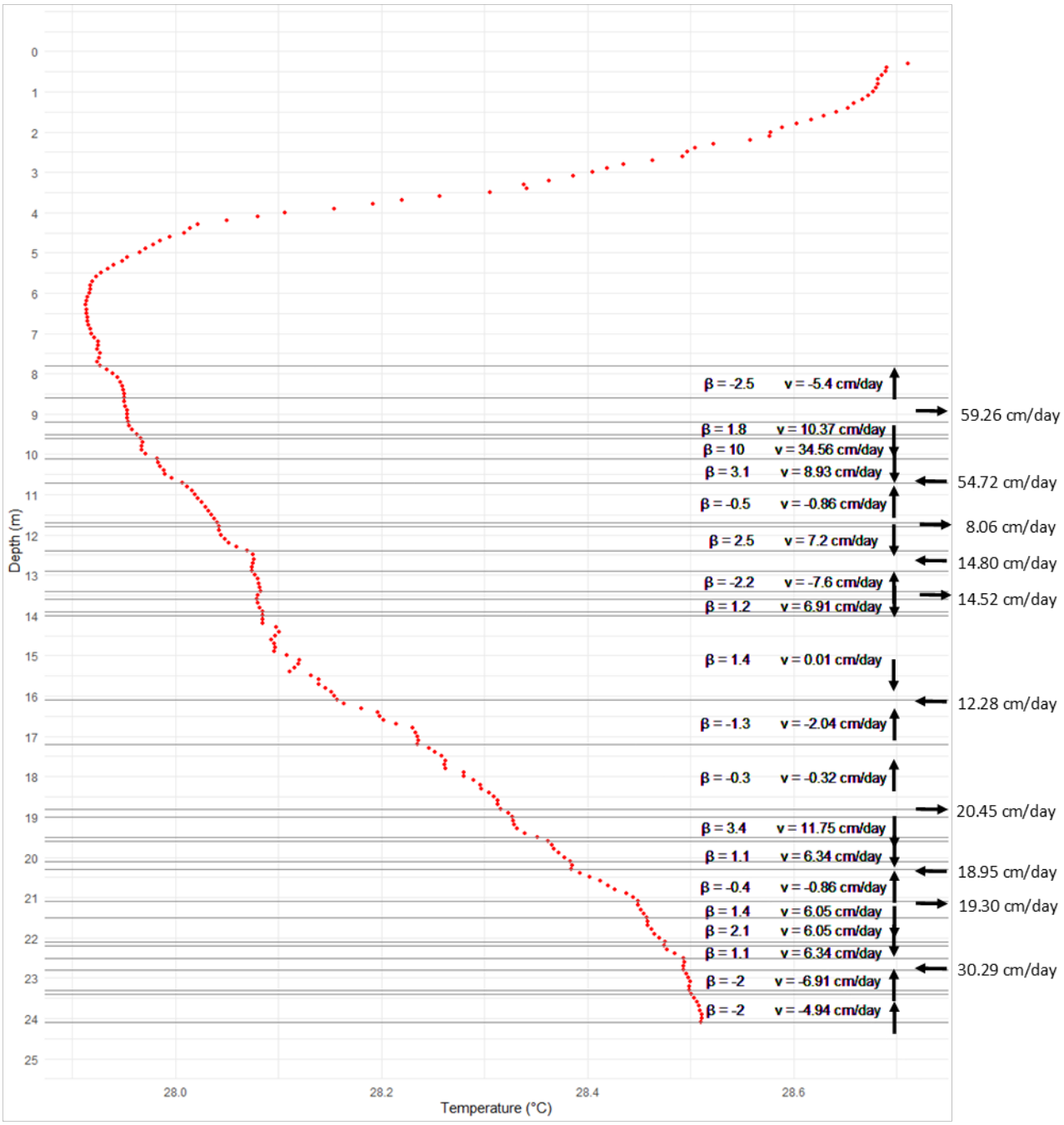

Figure 4.8: Static temperature-depth profile from well 7. Parameter β, fitted to the Bredehoeft and Papaopulos [1965] curves, is indicated for the areas marked by grey lines. With the calculated velocity next to it, where positive values mean upward movement and negative, downward. Vertical arrows point out the direction of flow, whereas horizontal arrows denote either into the well (to the right) or out of the well (to the left) flow from lateral sources with the cumulative flow indicated next to it.

4.1.2 Electrical conductivity depth profiles

Just as the temperature profiles, the electrical conductivity (EC) depth profiles can give an indication of fracture depths due to steps within the profile.

Well 3 (Figure 4.9) has one very straight line of around 3000 micro Siemens per centimeter. Only, at around 15.5 meters deep a big step is present, which is at the same depth as in the TD profile (where it was a small step). The other small step noted down for the TD profile at 7.5 meters is not visible in this profile.

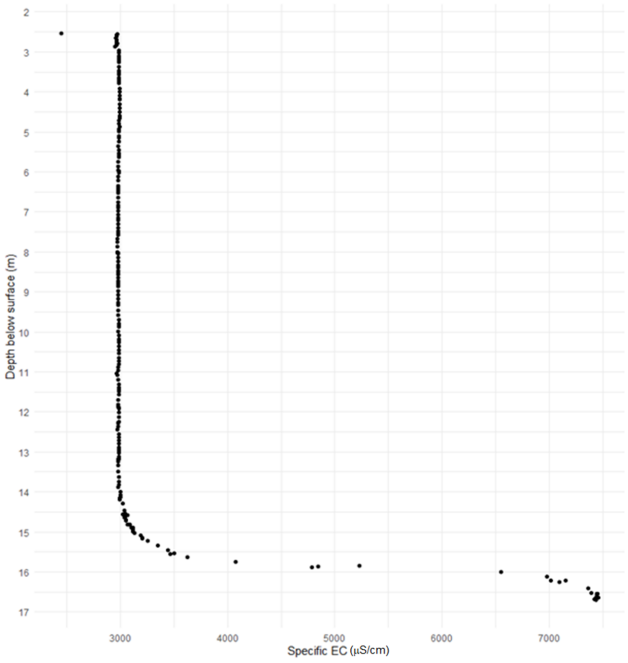

Figure 4.9: Specific EC in µS/cm in depth of well 3.

Figure 4.10 gives the profile of well 5, here steps can be noted down at the depths: 15.5, 20, 24 and 39 meters. Which is roughly the same depths as in the TD profiles shown in the former section, again also displaying wider steps at the top of the well and narrower at the bottom.

Well 6, in figure 4.11 depicts a few notable steps. These are around the depths of: 19, 31 and 35 meters, with the step at 19 meters being much wider than the other two steps. Here the surrounding influence of the fractures is higher.

The profile of well 7 (Figure 4.12) is more chaotic than previously shown profiles. The electrical conductivity within the well only differs between 1665 and 1695 µS/cm which is a small difference. At the depths of around 7.5, 11, 16, 18 and 20 meters the profile curves which could be a fracture depth, but not as clearly visible as steps as in the profiles shown beforehand. The

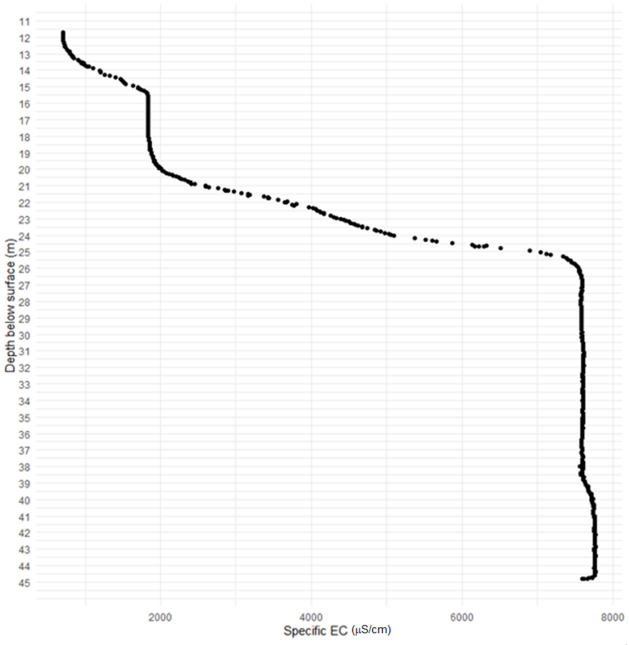

Figure 4.10: Specific EC in µS/cm in depth of well 5.

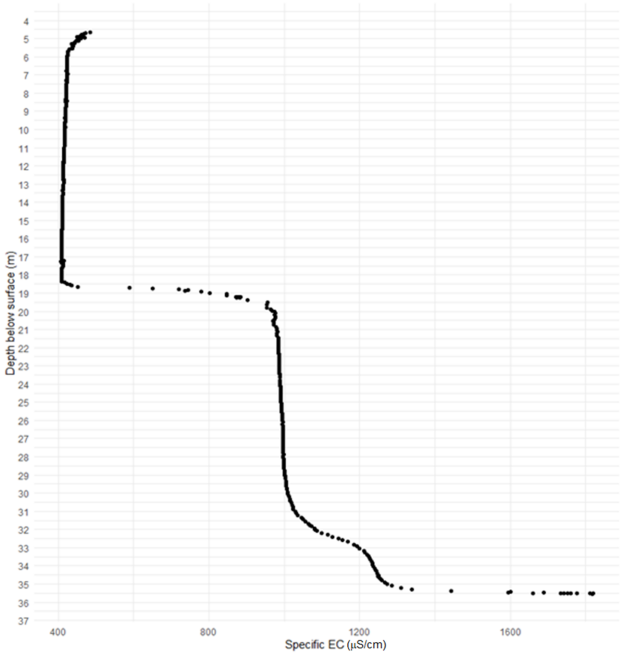

Figure 4.11: Specific EC in µS/cm in depth of well 6.

bottom of the well shows a lower value then the few meters above it just as in well 8.

Just as for the Temperature profile of well 8, the EC profile of this well (Figure 4.13) shows small differences within the whole depth. Again showing a decline near the bottom of the well at 7 meters deep, but only a slight difference of 100 µS/cm.

The profile of well 9 in figure 4.14 displays some significant steps with wider steps in the upper part of the well

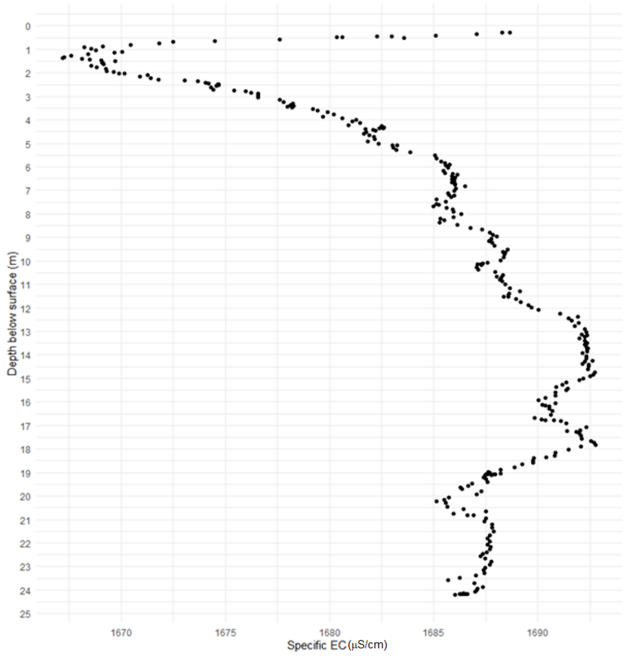

Figure 4.12: Specific EC in µS/cm in depth of well 7.

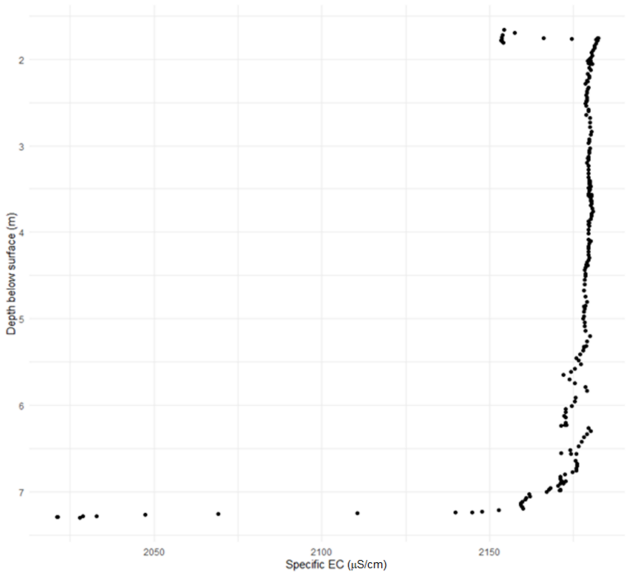

Figure 4.13: Specific EC in µS/cm in depth of well 8.

and smaller steps near the bottom. Steps are located at the depths of: 3, 8.5, 11 and 12.5 meters.

Figure 4.15 shows the EC profile of well 10, with a wide step around 13.5 meters and a small step near the bottom at 34 meters. These depths are comparable to the depths noted down for the TD profile of the same well. Again, the top fracture shows a wider step indicating higher influence from the surrounding.

Well 11 shown in figure 4.16 has a few steps. These steps are around the depths of: 11.5 and 19 meters, with the first being a wider step. The mentioned steps are around

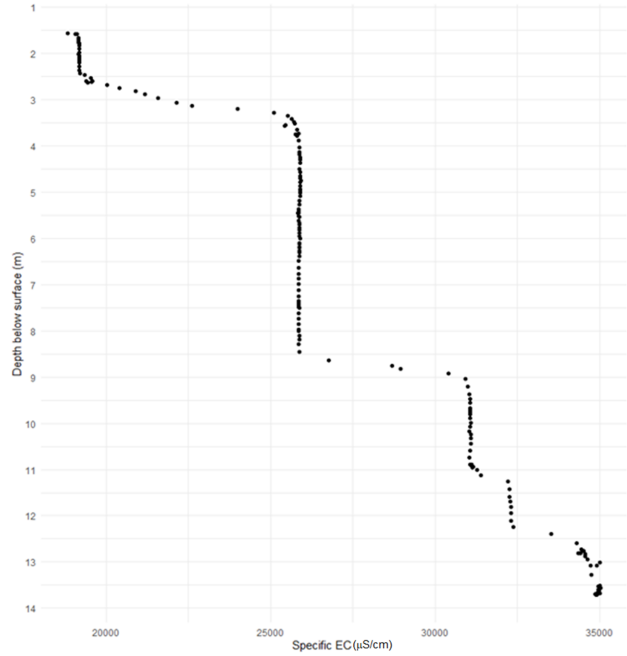

Figure 4.14: Specific EC in µS/cm in depth of well 9.

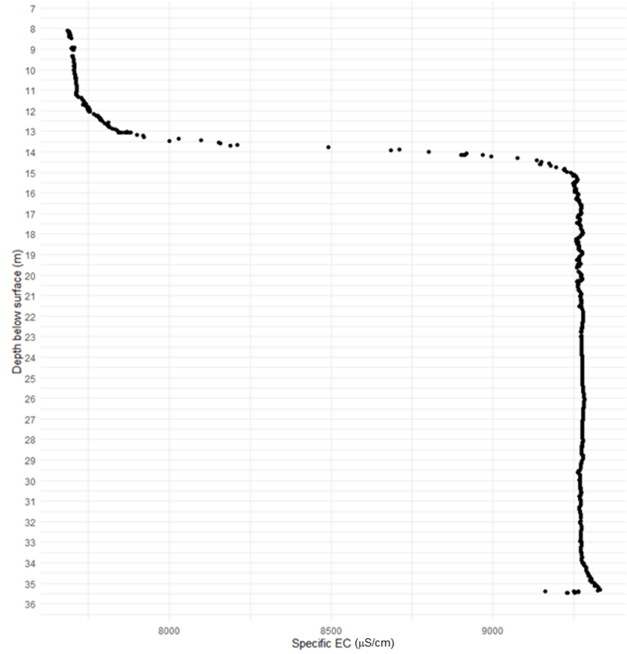

Figure 4.15: Specific EC in µS/cm in depth of well 10.

the same depths as noted for the TD profile.

4.2 Pump test profiles

Pump test were conducted to see whether the fracture depths noted for the static profiles, also are deducible during tracer tests, and if these tests could tell us more about these fractures. Here the different measuring techniques are also compared. Only the figures from the

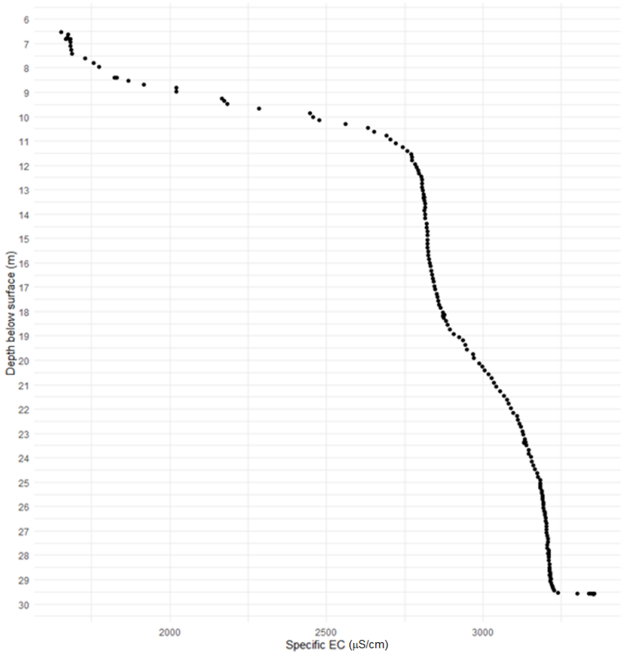

Figure 4.16: Specific EC in µS/cm in depth of well 11.

wells 7 and 9 are shown due to time constraint or data insufficiency. The plots of the other wells are given in appendix B.

4.2.1 Temperature tracer test

In the profiles presented in figure 4.17 from well 7, deviations from the background profiles can be noticed. The first thing noticeable is the heat plume that is created by the heater. The plume travels upwards dispersing its high temperature. In the figure the temperature difference from the first profile is presented. The deviations from the background profile show depths where lateral influence is present, thus fractures are present. Noted in the figures are the depths at which this happens, in figure 4.17 B, these depths are 8.5, 12.5, 14.2, 14.8, 16.5, 17.2, and 20.2 meters (dashed lines). Figure 4.17 A also shows the slope of the maximum temperatures of each Star Oddi temperature measurement line. The depths at which these velocities stagnate are 16.5 and 20.5 meters which roughly coincide with the depths indicated in figure 4.17 B. Another thing to note is that between 14 and 17 meters the profile is slightly warmer than the start, before the heater is turned on.
Figure 4.18 shows the same plot but for a different pump test, this is from well 9. This well was a bit shallower which is noticeable in the top Star Oddi temperature measurement line as it gives a lot of fluctuations in temperature. This because this Star Oddi was placed at the depth of the pump and is in contact with the temperature from the atmosphere. Again, depths with deviations from the background profiles are noted by dashed lines in figure 4.18 B. These are at depths of: 8.7, 10.2, 10.8, 12, 14.2, and 15 meters. In figure 4.18 A, the depths of interest are 10, 13, and 14 meters as the slope changes. Except for the 13 meters these depths coincide with the found depths in figure 4.18 B.

To illustrate the possibilities of velocity calculations the profiles from well 9 are plotted again, but this time with the temperature on the x-axis in figure 4.19. Slopes of selected consecutive profile's maximum temperatures have been calculated and plotted (excluding maximum temperatures occurring above the pump depth). What is notable is the velocity change around 14.2 meters, below this the flow is 0.63 l/min where above it is 0.33 l/min, which is almost half of the speed from below. This indicates lateral influence, as the flow stagnates in the well, meaning the flow from below is dissipating out of the well. This figure also again shows the depths of interest mentioned before in figure 4.18.

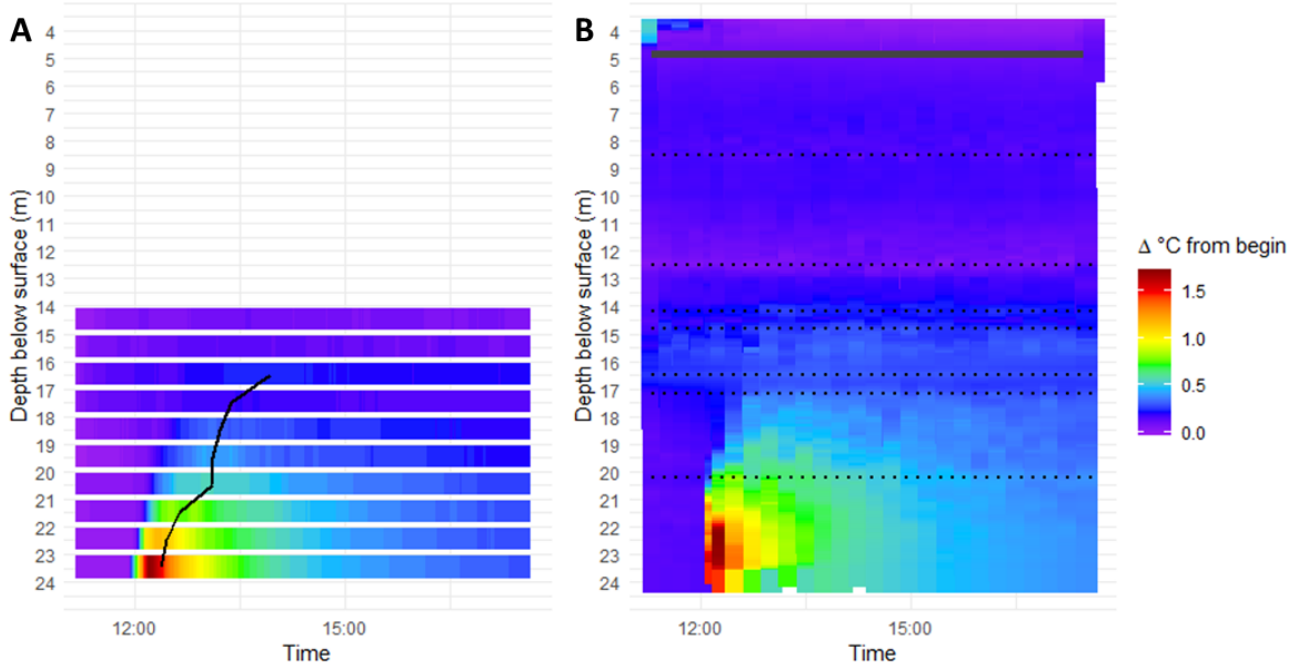

Figure 4.17: the temperature difference from the first profile (before pumping) in depth and time from the pump test in well 7. Measurements from the Star Oddi's in A and the CTD logger in figure B. The black lines in figure A depict the slope between the maximum temperatures from each Star Oddi, where minus is upwards. The grey line in figure B indicates the depth of the pump at the times that the pump was active, and the dashed lines indicate the depths at which proposed fractures are present

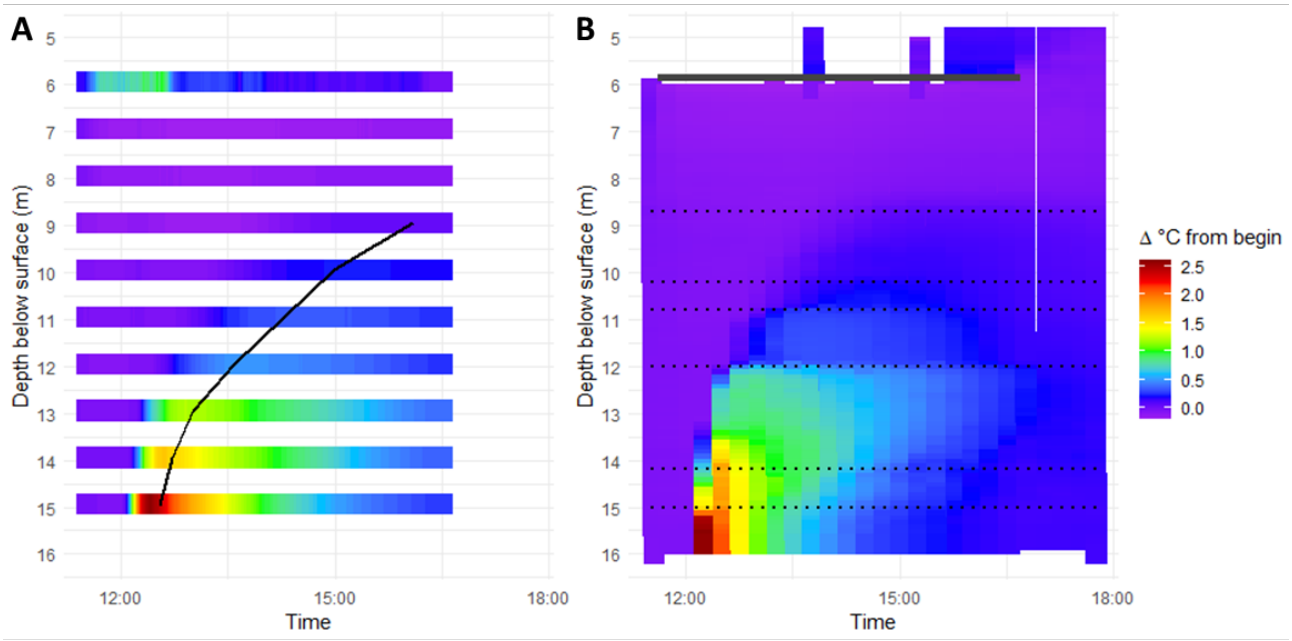

Figure 4.18: the temperature difference from the first profile (before pumping) in depth and time from the pump test in well 9. Measurements from the Star Oddi's in A and the CTD logger in figure B. The black lines in figure A depict the slope between the maximum temperatures from each Star Oddi, where minus is upwards. The grey line in figure B indicates the depth of the pump at the times that the pump was active, and the dashed lines indicate the depths at which proposed fractures are present.

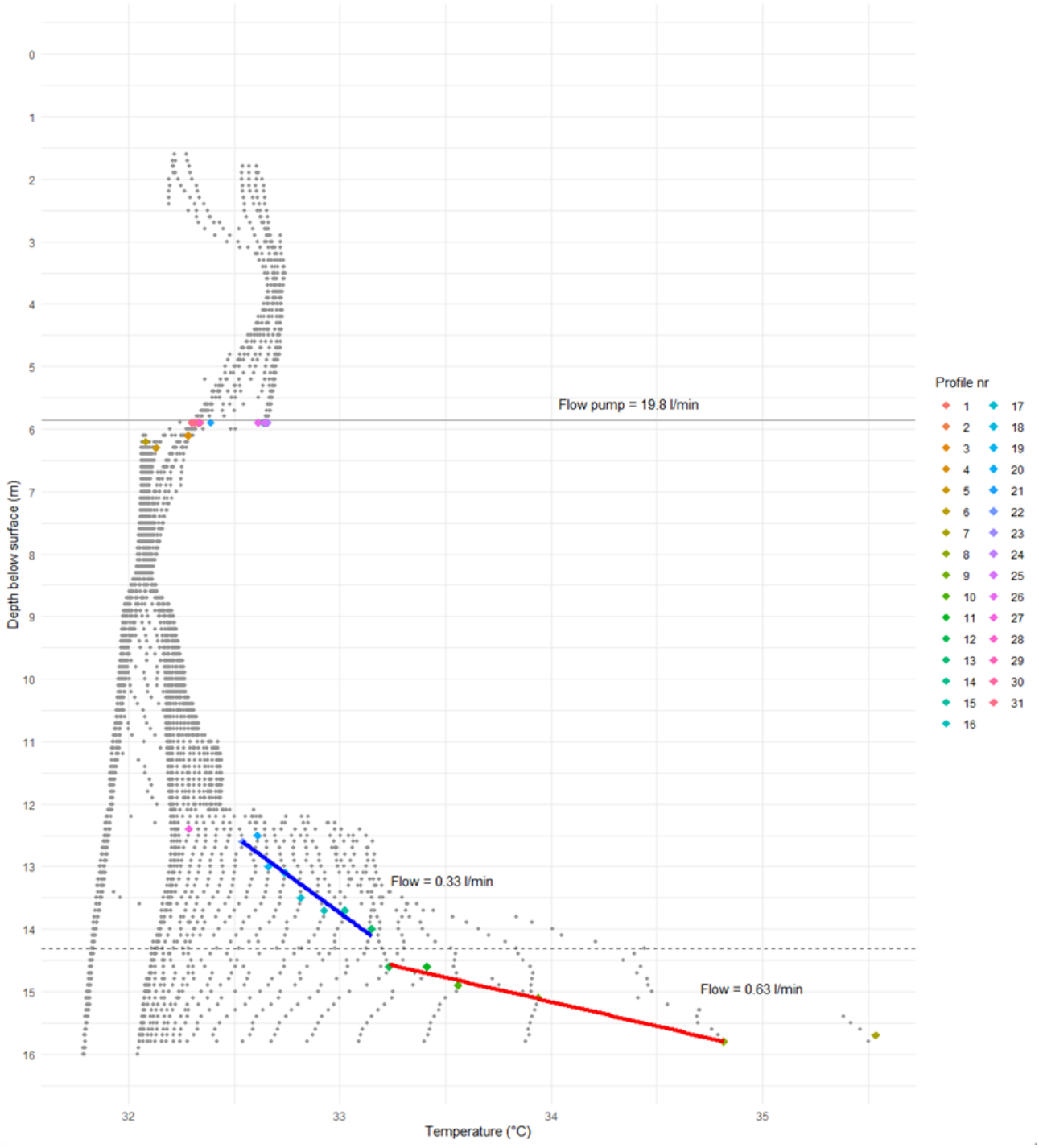

Figure 4.19: all profile Temperature measurements from the pump test in well 9. Coloured diamonds are indicators of the highest temperature of each profile, where the blue and red lines depict the calculated slopes of selected sections. The red line is the maximum temperatures of profiles 8 to 12 and for blue 13 to 22. The flow velocity of these sections is indicated above the lines, which is calculated using the time it took the maximums to rise the depth difference of the section. The pump flow velocity is indicated above the grey line which indicates the pump depth.

4.2.2 Salt tracer test

The following figures will present the measured EC profiles from the pump tests in well 7 (Figure 4.20) and well 9 (Figure 4.21). For these measurements, no external tracer injection was used. Figure 4.20 shows the difference in specific EC from the first profile. Where the grey line is the height of the pump and stretches from the start to the end of the pump session. The average EC value is around 1700 µS/cm (Appendix figure A.1). Noticeable deviations from the background profiles are marked with a dashed black line. These are at the depths of, 9.7, 12.5, 15.5, 17.2, 20.4, and 22.4 meters, which are comparable with the temperature tracer test depths. Notable in this profile, is the input of lower EC values from the bottom halfway through the test, which slowly move upwards as pump time passes. In the static profile of this well, already a lower EC value is seen near the lower depths of the well (Figure 4.12). For well 9 the profiles are presented in figure 4.21. The overall EC in this well was around 30000 µS/cm (Appendix figure A.2). Which is more than 15 times the amount of well 7. The dashed lines in this plot are at the depths of 8.5, 10.2, 10.8, 12, 13.5, 14, and 15.2 meters, which are comparable with the temperature tracer test depths. With depths of 8.5, 10.8, and 12 meters show the most influence as the most difference is visible here.

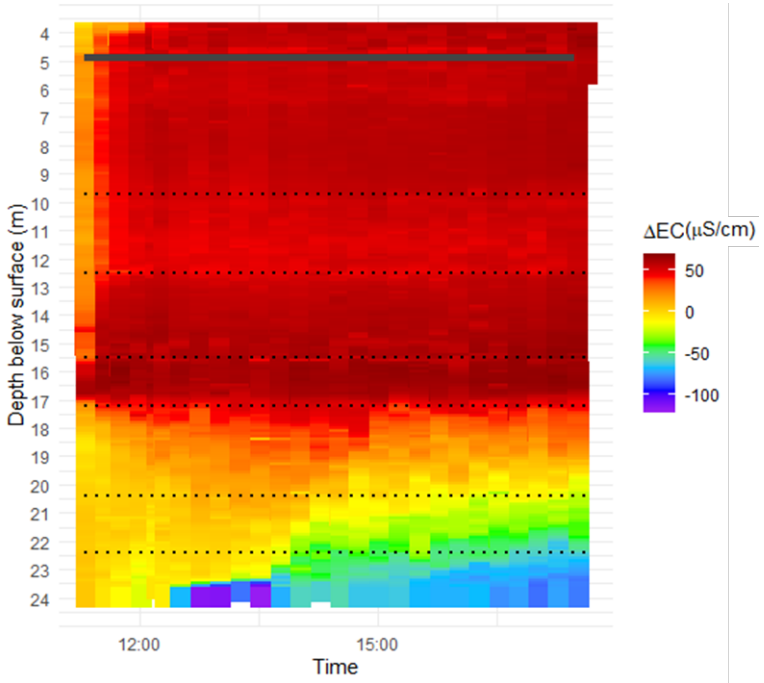

Figure 4.20: Specific EC in µS/cm difference from the first profile (before pumping) in depth and time of well 7. The grey line indicates the pump depth. The dashed lines indicate depths at which proposed fractures are present.

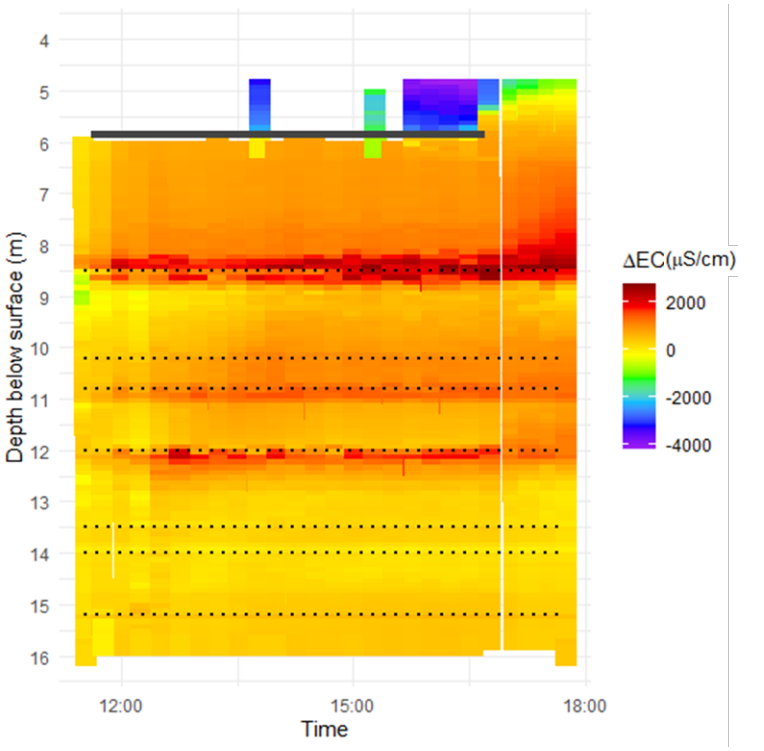

Figure 4.21: Specific EC in µS/cm difference from the first profile (before pumping) in depth and time of well 9. The grey line indicates the pump depth. The dashed lines indicate depths at which proposed fractures are present.

5 | Discussion

In this chapter, the results will be discussed. Firstly, the static measurements will be examined, with temperature and conductivity handled separately. Following that, the discussion will move to the pump test measurements.

5.1 Static profiles

The static temperature depth (TD) profiles overall show some steps and irregularities along the profiles suggesting fractures, especially in the TD profile of well 5 (figure 4.2). In this profile distinguishable steps are visible. This is also the only profile from the Midden Curaçao formation which has a much lower transmissivity than the Curaçao lava formation. It can be hypothesised that the heat transfer between layers differs and thus, because of the different geological stones such as sand or mud stones, the heat transfer upwards in the profile is slowed down by lower transmissive layers. For the other wells no such clear steps were visible but more irregularities were noted done as fracture depth.

Because only one profile is analysed per well, some uncertainty is added, as it is a snapshot measurement. This influences the static profile analyses done for well 7 (Figure 4.8). As this analyses is done on small areas of the profile. Small temperature deviations can have a bigger impact on the result. As not the whole profile showed distinguishable curves to assess with the Bredehoeft curve's, a section of 5 meters (between 14 and 19 meters) could not be given flow velocity for each subsection within this section. Thus within this region of the profile small deviations can cause a currently presented upward flow to flow downwards or cause a different magnitude of flow velocity. Some uncertainty is also present in the magnitude of the velocity since the well diameter, which is used in the velocity calculation, is not homogeneous throughout the well. This was noticed after taking an in-well video showing ridges and imperfections created by the drilling of the well. As these diameter deviations are quite aprubt and diverse throughout the well the diameter of the well was assumed to be uniform over the whole depth. The measured diameter at the top was chosen to represent the diameter of the entire well. To diminish this effect in further research, a more intense investigation on these deviations is necessary to get more accurate velocities.

For the electrical conductivity (EC) profiles, steps in µS/cm were more distinguishable in the presented profiles, and thus proven use full in finding fracture depths. This conclusion is similar to what Saxena et al. [2005] found in the subsurface of India. Except for the profile of well 7 and 8 where the difference of EC within the profile is no more than 100 µS/cm. Well 7 is roughly 1.2 km away from well 6 which has a much lower general EC value, around 1000 µS/cm instead of 1680 for well 7, and showcases better distinguishable steps in the profile. Wells 6 and 7 showcase that the connectivity between the wells, hypothetically is not high, as it does not show comparability among the two profiles. Also for wells 9 and 10 this EC value difference is present as the general values within these wells are around 27500 µS/cm for well 9 and 8500 µS/cm for well 10. These wells lie again roughly 1.2 km apart from each other and at almost the same height but have a big difference in magnitude of µS/cm. Which with looking at figure 1.3 again enhances the idea of heterogeneity within the island as both wells are almost as close to the coast but have very different characteristics. The hypotheses here is that well 9 probably has a connection to the sea water as it shows such high values compared to well 10.
In general the wells, except for well 7 and 8, show smaller steps as the depth of the well increases. Which would suggest that the weathering of the subsurface rock and thus fracture formation is diminished with depth. And that this process is seen across the island within the Curaçao lava formation. Wells 7 and 8 did not follow this pattern as lower EC and temperature values are present at the bottom of the wells. Well 8 lies near some lakes which could explain the lower values at the bottom of the well, assuming there is some kind of connectivity between the bottom of the well and the available water nearby. To investigate this further, water from the bottom of the well could be tested to see if it resembles values from the lake water. For the other geological formations only one or no profiles were analysed or measured and thus remains outside of this discussion point, but is an interesting topic of future research.

5.2 Temperature tracer test

As general notes on the temperature experiment side of the pump tests, the heater is only turned on at the bot-

tom of the wells. This restricts the analyses as done in figure 4.19 for multiple depths as the heat plume is dissipated above 12.5 m. Above this the maximum temperatures caused by the heat plume can not be detected. To get a more detailed picture of the whole fracture distribution in the well, this test should be repeated with the heater at different depths or with a longer heating time. Overall the temperature tracer test did show significant results in detecting fracture depths, at the depths that the heat plume did travel. As Leaf et al. [2012] and Read et al. [2015] states this method is use full in detecting fracture depths, where in their study they did use a DTS (distributed temperature sensing) system to mitigate the disturbing of the profile by pulling the logger up and down the well, as was used in this study. In future research, when available, DTS can be used for a less disturbed continuous temperature measurement.

For the measurements of temperature, both Star oddi's and the RBR Brevio[3] were used. Here both measurement and analysis methods will be discussed.

5.2.1 Star Oddi's

The indicated depths of interest discussed in the results section in figure 4.17 en 4.18 are based on the slope of the highest temperature differences per Star Oddi. As the Oddi's were placed every meter the exact depth of the fracture that forces this slope change is unsure. Thus these could vary within the surrounding one meter at each side of the indicated Oddi. If an analysis of higher detail is needed in further research, a more dense Oddi placement is required. Also, as only ten Star Oddi's were available not the whole extent of every well could be monitored. To get a conclusive picture of the full extent of a well more Oddi's would be needed to be placed along the depth. Another point to be raised is that possible small deviations in temperature could be present between two Oddi's which do not show up in the bigger scale of measurements. Such a thing is seen in figure 4.18 A as at 12 meters depth, nothing can be noted and in figure 4.18 B a clear line is visible. Thus a method with these one meter spacing of Oddi's as measurement device does not result in a complete overview of the fractures present in a well but it does give a more continuous measurement throughout the test than the CTD logger data and a general idea of the situation within the well.

5.2.2 Temperature depth profiles

Same as for the Star Oddi temperature measurements, in the temperature depth profiles the plume is dissipated before the top of the well. For well 7 shallow depths are mentioned to have a clear difference from the background profile at 8.5 and 12.5 meters. The heat plume does not have impact on these depths. At these depths the influence of lateral groundwater changes the measured start temperature. These changes are thus only induced by pumping. This phenomenon only showcases the depths where the input temperature (lateral groundwater temperature) is different from the start well temperature. To know whether there are also fractures at depths with the same temperature as this starting temperature the heat plume experiment should be done at higher depths. Read et al. [2015] also noted this as a complication of the method.

For the calculation of flow in figure 4.19 the height of the temperature plume is used with the speed of which it has moved up times the diameter of the well. Poulsen et al. [2019] however does this with a tracer test where there is a constant tracer input. Thus the shown calculated flows do not depict the correct magnitude of velocities, but it does however indicate a change of flow between the two lines, which indicates a lateral inflow point. When wanting to know the correct flow velocity future studies could redo the pump test with a constant temperature input.

Uncertainty was induced by snapshot measurement of the first temperature profile. The analyses done for the temperature depth profiles are plotted as the difference of the measured temperature of the profile with the first full profile before a pumping test. This could have impact on the outcome, as if at any depth a small temperature difference occurs for a few seconds during the first profile, it can have impact on the results. To diminish this, multiple start profiles should be taken and averaged. These profiles should be taken with some time in between to diminish the temperature flow induced by the dropping an pulling up of the CTD-logger.

When looking at the figure 4.17 as noted, parts of the profile were heated up before turning on the heater. This heat thus is transported trough lateral inflow of groundwater. As it is heating up the profile, this water has to originate from either higher or lower parts of the subsurface as as seen in figure 4.8 in those places the water is of higher temperature.

For well 9 this is not the case and seems, temper-

ature wise, only affected by lateral inflow after heating at the noted down depths. These depths are comparable to the depths from the static profiles, but do give more notable fracture depths. It could be hypothesised that the depths at which no steps are seen in the static profiles but only in the pump test, that the fractures are not connected to a bigger flow path where surrounding water can enter but is a pocket that holds some water. This effect could potentially be analysed by taking a longer pump test to see if the effect of these hypothetically non connected fractures diminishes over time.

5.3 Salt tracer test

As proposed in the methods, the EC concentration from the bottom of a well could be used as natural tracer. In figure 4.20 about halfway the test, the EC is pulled upwards due to the pumping. This induced flow visualised the fracture depth of 20.4 and 22.4 meters. Where this effect is not seen in the others wells. Well 7 is also different from the other wells as the EC concentration in the bottom of the well is lower than at the top. Moreover, the movement upwards of this fresher water starts after the heat plume has past. As convection of the warmer groundwater is flowing upwards the inflow of lateral groundwater is induced, which in this case has a lower EC concentration. This fresher water could be originated from surrounding surface water that has a flow path to these lower depths. Potentially this water can originate from either the, potential leaking, water basin nearby or the water standing at the dam. This could be investigated by taking a water sample at the bottom of the well and comparing it with the surrounding water sources.
Well 9 does not showcase the same as well 7. In this pump test the higher EC values did travel upwards in the well and stagnated at the noted depths were the lateral inflow causes dilution of this upwards flow. Again, as noted with the heat tracer test the noted depths are comparable with the depths of the steps in the static profiles but did give more notable depths. These extra depths (such as 10.2, 14 and 15 meters) do show less of an influence in the profile, thus probably do also have less impact on the surrounding groundwater flow than the other depths (8.5, 10.8 and 12 meters).

Furthermore, the impact of snapshot measurements of the first full EC profile is potentially affecting the outcome. In the same manner as for the temperature profiles, the small possible deviations of the measured EC concentration can have impact on the conclusions made from the figures 4.20 and 4.21. In future use of this method, the assumption of the first profile being correct as a snapshot measurement can be diminished by averaging multiple profiles taken before pumping with time in between. Overall, did this natural salt tracer method prove to be use full in locating fractures in a single well tracer pumping test.

6 | Conclusion

The aim of this research around Curaçao was to investigate fractures in the geological subsurface of the island. This was done using conductivity temperature depth (CTD) profiles while preforming a tracer pump test. The fractures in the subsurface of Curaçao can be characterised by analysing CTD profiles during multiple types of tracer pump tests in a well: either by conducting a natural tracer test within a well with a non-uniform electrical conductivity (EC) profile or by a point source heat injection. Illustrating the difference of each CTD profile from the initial static profile exposed deviations, after which were assumed to indicate fracture depths. Both the temperature and EC experiments show comparable depths of these fractures. The results also provide more insight in the heterogeneity of the subsurface of the island, as the connectivity between wells is low and the fracture density diverse. In addition it was found that the fracture density decreases with depth.

The proposed methods demonstrate effectiveness in their respective capacities. Static CTD profiles have shown comparable fracture depths between each other (temperature and EC) and to the tracer tests. However, a more insightfull fracture distribution can be seen with the CTD profiles of the tracer tests, which in some cases more information was revealed due to prolonged pumping. Furthermore, the Oddi measurement method shows promising results but proves to be less effective at the current measurement density. When using a method involving temperature point source injection as a tracer, it is advisable to conduct multiple injections at varying depths of interest to enhance result accuracy. Future research could investigate the relationship between the different geological formations better by conducting additional tests within different formations. To conclude, natural tracer tests with EC in coastal formation can be an insightfull and an effective method, where static CTD profiles can already provide a good estimation of fractures in a well.

Acknowledgements

First I want to thank my supervisors Victor Bense and Titus Kruijssen for helping me with this project and giving me the change to make my master thesis. I also would like to thank Mike Wit, Titus Kruijssen and Joshua Leusink for an amazing fieldwork trip, and the fun we had on the island and at Carmabi. Also big gratitude towards the well owners on the island for letting us do fieldwork on their lands, where even sometimes multiple times. Also many thanks for Carmabi for providing us housing and accessibility to labs and the amazing people in residence at that time. Lastly, I want to thank all the MEE master thesis students for the great feedback during the thesis rings and in the thesis room.

Bibliography

Bernd Abtmaier. *Zur Hydrogeologie der Insel Curacao (Niederländische Antillen)*. Rheinische-Westfälischen Hochschule Aachen, Facultät für Bergbau und Hüttenwesen, 1978.

DJ Beets. Lithology and stratigraphy of the cretaceous and danian succession of curacao (ph. d. thesis): University of amsterdam. *The Netherlands*, 1972.

J D Bredehoeft and IS Papaopulos. Rates of vertical groundwater movement estimated from the earth's thermal profile. *Water Resources Research*, 1(2):325–328, 1965.

Tyler D Eddy, Vicky WY Lam, Gabriel Reygondeau, Andrés M Cisneros-Montemayor, Krista Greer, Maria Lourdes D Palomares, John F Bruno, Yoshitaka Ota, and William WL Cheung. Global decline in capacity of coral reefs to provide ecosystem services. *One Earth*, 4(9):1278–1285, 2021.

Robert M Gailey. Inactive supply wells as conduits for flow and contaminant migration: conditions of occurrence and suggestions for management. *Hydrogeology journal*, 25(7):2163, 2017.

Andrew T Leaf, David J Hart, and Jean M Bahr. Active thermal tracer tests for improved hydrostratigraphic characterization. *Groundwater*, 50(5):726–735, 2012.

Michael P Lesser. Eutrophication on coral reefs: what is the evidence for phase shifts, nutrient limitation and coral bleaching. *BioScience*, 71(12):1216–1233, 2021.

Joshua A.E. Leusink. Pump it up: investigating the hydrogeologocal properties of curaçao's subsurface. *Master thesis*, 2024.

Jianan Liu and Jinzhou Du. Submarine groundwater discharge impacts on marine aquaculture: A mini review and perspective. *Current Opinion in Environmental Science & Health*, 26:100325, 2022.

Katie A Lubarsky, Nyssa J Silbiger, and Megan J Donahue. Effects of submarine groundwater discharge on coral accretion and bioerosion on two shallow reef flats. *Limnology and Oceanography*, 63(4):1660–1676, 2018.

Albert Martis, Geert Jan van Oldenborgh, and Gerrit Burgers. Predicting rainfall in the dutch caribbean—more than el niño? *International Journal of Climatology: A Journal of the Royal Meteorological Society*, 22(10):1219–1234, 2002.

L Maurice, JA Barker, TC Atkinson, AT Williams, and PL Smart. A tracer methodology for identifying ambient flows in boreholes. *Groundwater*, 49(2):227–238, 2011.

Meteorological Department Curaçao. URL `https://www.meteo.cw/climate.php?Lang=Eng&St=TNCC&Sws=R11`. [Accessed 24-04-2024].

Vincent EA Post, Amandine L Bosserelle, Sandra C Galvis, Peter J Sinclair, and Adrian D Werner. On the resilience of small-island freshwater lenses: Evidence of the long-term impacts of groundwater abstraction on bonriki island, kiribati. *Journal of Hydrology*, 564: 133–148, 2018.

David L Poulsen, Peter G Cook, Craig T Simmons, James M McCallum, Saskia L Noorduijn, and Shawan Dogramaci. A constant rate salt tracer injection method to quantify pumped flows in long-screened or open borehole wells. *Journal of Hydrology*, 574: 408–420, 2019.

T Read, Victor F Bense, R Hochreutener, O Bour, T Le Borgne, N Lavenant, and JS Selker. Thermal-plume fibre optic tracking (t-pot) test for flow velocity measurement in groundwater boreholes. *Geoscientific Instrumentation, Methods and Data Systems*, 4 (2):197–202, 2015.

R.J. Rowbottom and C.W. Winkel. Groundwater investigation curaçao. *Department of Agriculture Curaçao*, 1979.

VK Saxena, NC Mondal, VS Singh, and Dewashish Kumar. Identification of water-bearing fractures in hard rock terrain by electrical conductivity logs, india. *Environmental Geology*, 48:1084–1095, 2005.

Sealink. URL `https://www.sealinkcaribbean.net/`.

Brij Bhusan Saran Singhal and Ravi P Gupta. *Applied hydrogeology of fractured rocks*. Springer Science & Business Media, 2010.

C Christopher Smart and Stephen RH Worthington. Electrical conductivity profiling of boreholes as a means of identifying karst aquifers. In *Sinkholes and the Engineering and Environmental Impacts of Karst*, pages 265–276. 2003.

Gerard van Buurt. A short natural history of curaçao. In *Crossing Shifting Boundaries, Language and Changing Political status in Aruba, Bonaire and Curaçao. Proceedings of the ECICC Conference, Dominica*, volume 1, pages 229–256, 2009.

Waitt institute. The state of curaçao's coral reefs. *ASSESSMENT, MARINE SCIENTIFIC*, 2017.

NRG Walton. Electrical conductivity and total dissolved solids—what is their precise relationship? *Desalination*, 72(3):275–292, 1989.

A | Additional Figures

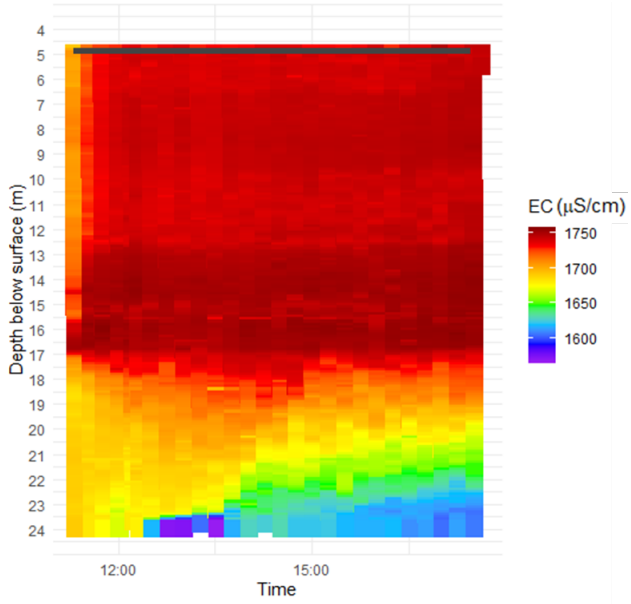

Figure A.1: Specific EC in µS/cm in depth and time of well 7. The grey line indicates the pump depth.

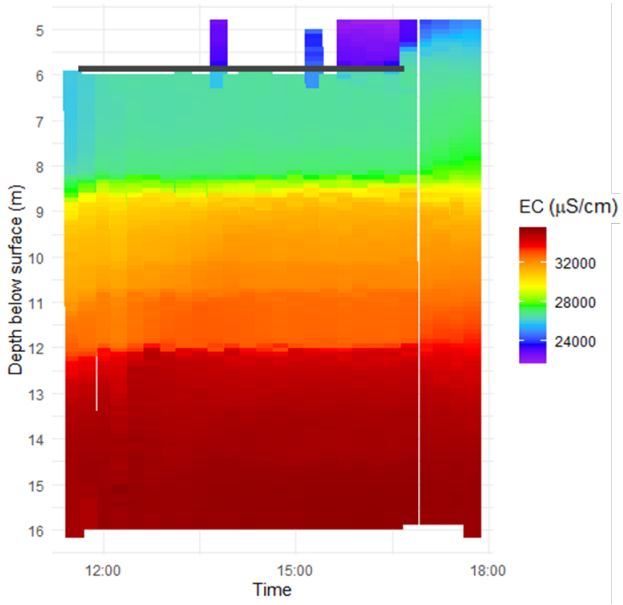

Figure A.2: Specific EC in µS/cm in depth and time of well 9. The grey line indicates the pump depth.

B | Figures non analysed wells

For wells 1, 2 and 4 in figure 2.2 either no data was present due to a too narrow well (4) or emptying the well directly after turning on the pump (1). For well 2 the data was logged with a diver instead of the RBR Brevio[3]

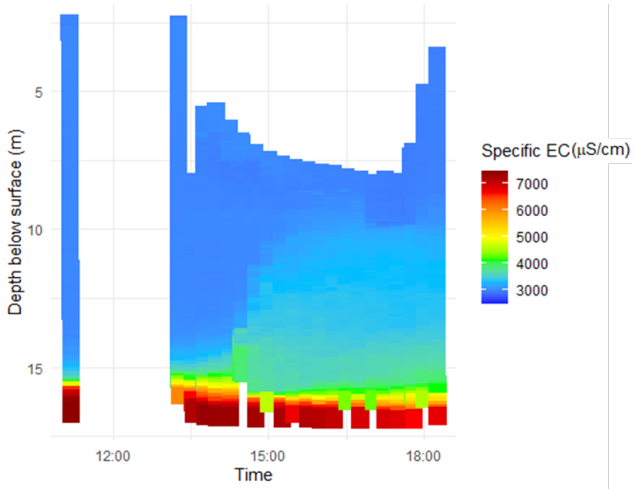

Figure B.1: Specific EC in µS/cm in depth, well 3 figure 2.2

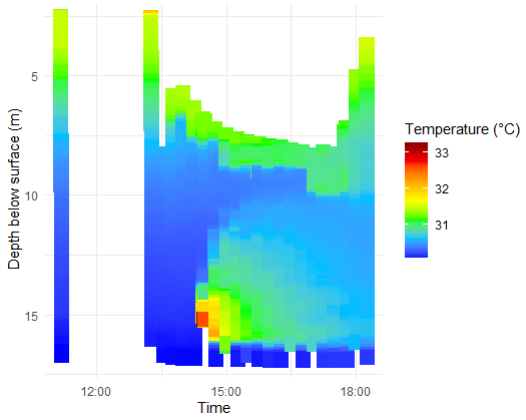

Figure B.2: Temperature in degrees in depth, well 3 figure 2.2

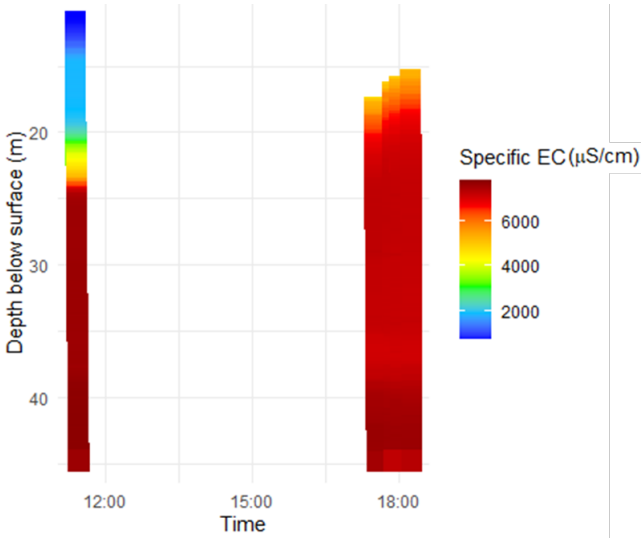

Figure B.3: Specific EC in µS/cm in depth, well 5 figure 2.2

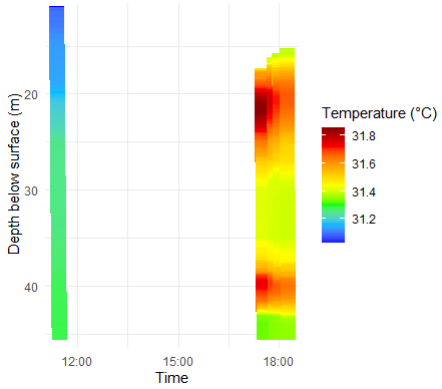

Figure B.4: Temperature in degrees in depth, well 5 figure 2.2

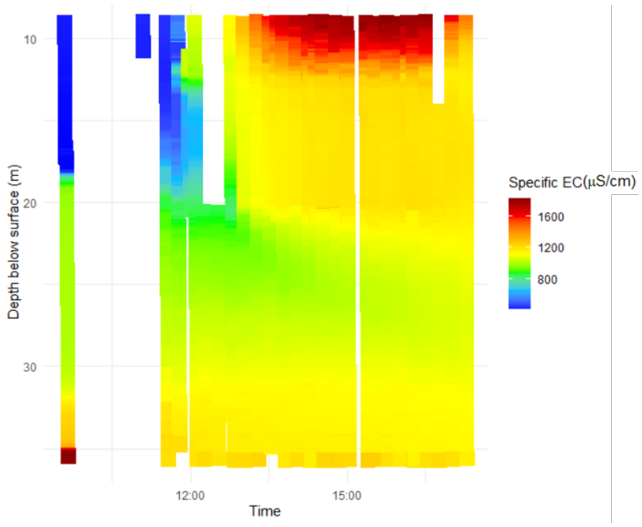

Figure B.5: Specific EC in µS/cm in depth, well 6 figure 2.2

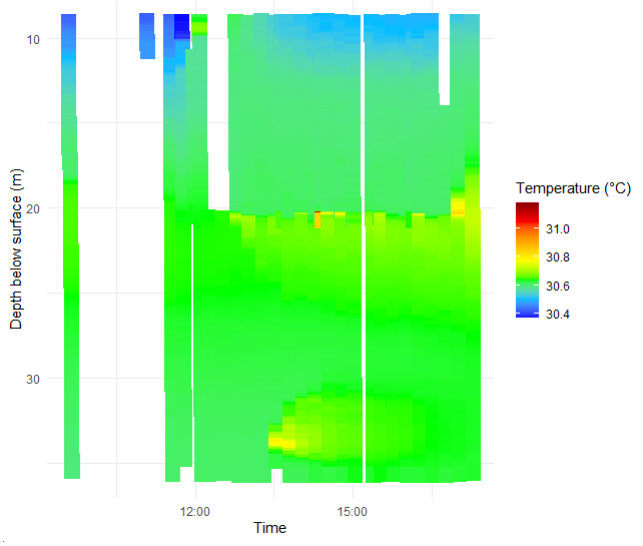

Figure B.6: Temperature in degrees in depth, well 6 figure 2.2

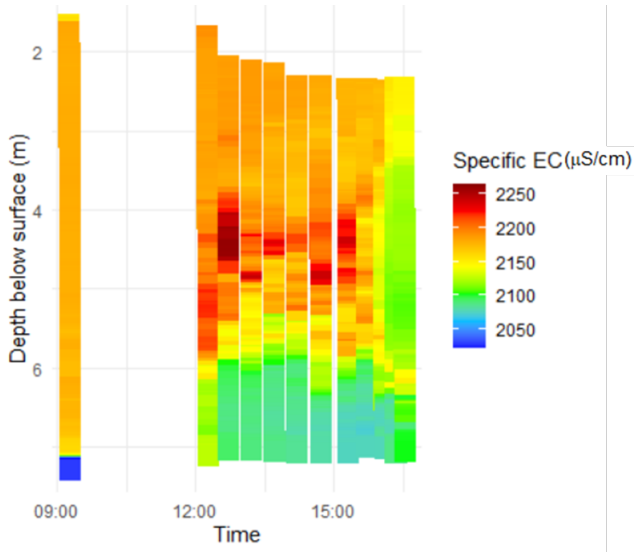

Figure B.7: Specific EC in µS/cm in depth, well 8 figure 2.2

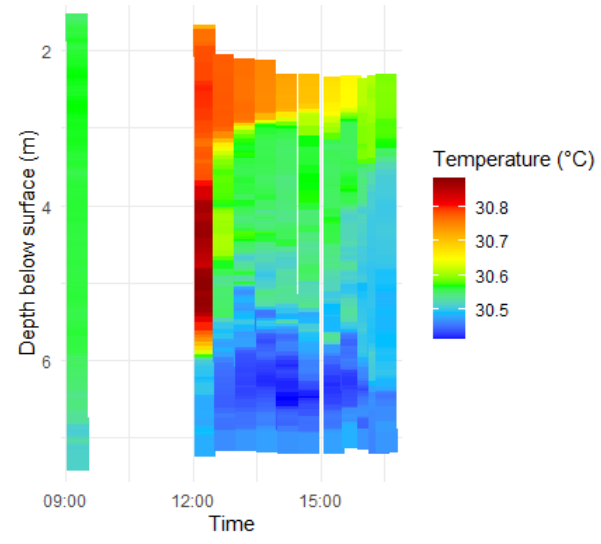

Figure B.8: Temperature in degrees in depth, well 8 figure 2.2

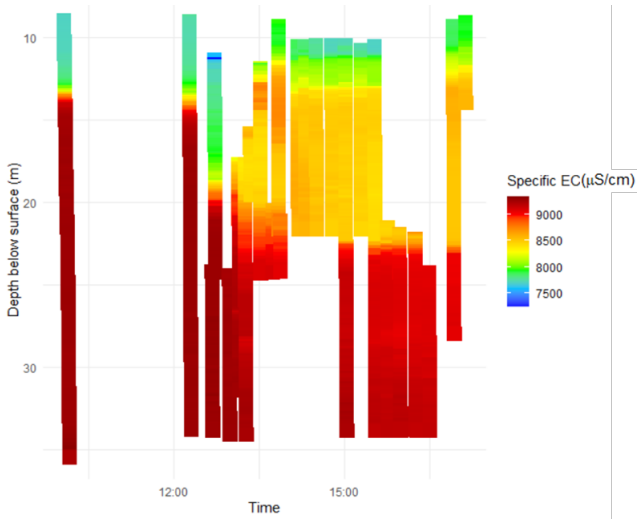

Figure B.9: Specific EC in µS/cm in depth, well 10 figure 2.2

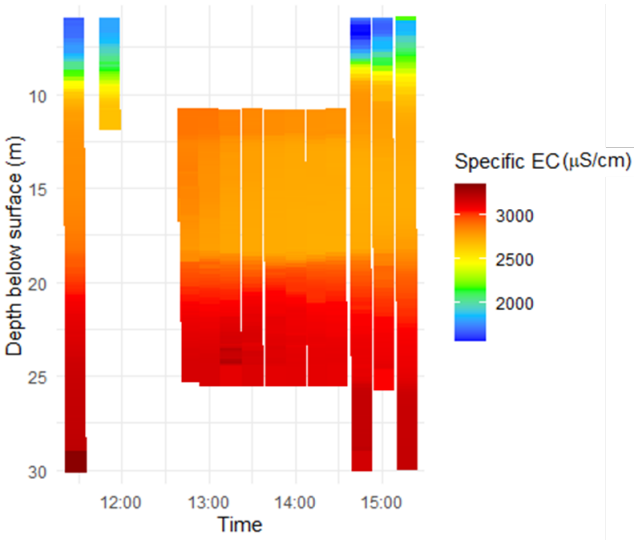

Figure B.11: Specific EC in µS/cm in depth, well 11 figure 2.2

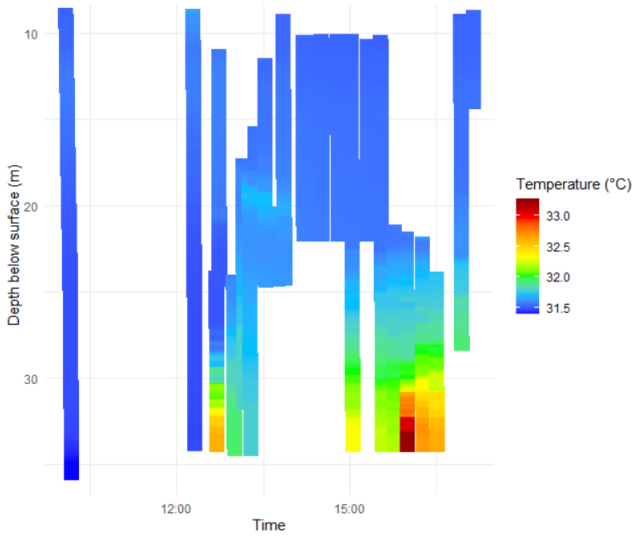

Figure B.10: Temperature in degrees in depth, well 10 figure 2.2

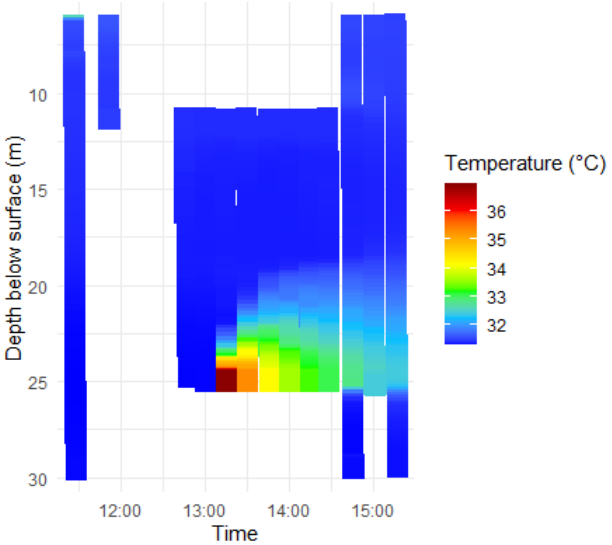

Figure B.12: Temperature in degrees in depth, well 11 figure 2.2